

## Accepted Manuscript

Structure characterization of one polysaccharide from *Lepidium meyenii* Walp., and its antioxidant activity and protective effect against H<sub>2</sub>O<sub>2</sub>-induced injury RAW264.7 cells

Wei Wang, Fenmin Zhang, Qian Li, Hui Chen, Weijie Zhang, Ping Yu, Ting Zhao, Guanghua Mao, Weiwei Feng, Liuqing Yang, Xiangyang Wu



PII: S0141-8130(18)31367-9  
DOI: doi:[10.1016/j.ijbiomac.2018.06.117](https://doi.org/10.1016/j.ijbiomac.2018.06.117)  
Reference: BIOMAC 9957

To appear in: *International Journal of Biological Macromolecules*

Received date: 22 March 2018  
Revised date: 22 June 2018  
Accepted date: 23 June 2018

Please cite this article as: Wei Wang, Fenmin Zhang, Qian Li, Hui Chen, Weijie Zhang, Ping Yu, Ting Zhao, Guanghua Mao, Weiwei Feng, Liuqing Yang, Xiangyang Wu, Structure characterization of one polysaccharide from *Lepidium meyenii* Walp., and its antioxidant activity and protective effect against H<sub>2</sub>O<sub>2</sub>-induced injury RAW264.7 cells. *Biomac* (2018), doi:[10.1016/j.ijbiomac.2018.06.117](https://doi.org/10.1016/j.ijbiomac.2018.06.117)

This is a PDF file of an unedited manuscript that has been accepted for publication. As a service to our customers we are providing this early version of the manuscript. The manuscript will undergo copyediting, typesetting, and review of the resulting proof before it is published in its final form. Please note that during the production process errors may be discovered which could affect the content, and all legal disclaimers that apply to the journal pertain.

**Structure characterization of one polysaccharide from *Lepidium meyenii* Walp., and its antioxidant activity and protective effect against H<sub>2</sub>O<sub>2</sub>-induced injury RAW264.7 cells**

Wei Wang<sup>a,1</sup>, Fenmin Zhang<sup>b,1</sup>, Qian Li<sup>a</sup>, Hui Chen<sup>c</sup>, Weijie Zhang<sup>a</sup>, Ping Yu<sup>d</sup>, Ting Zhao<sup>d</sup>, Guanghua Mao<sup>c</sup>, Weiwei Feng<sup>c</sup>, Liuqing Yang<sup>d\*</sup>, Xiangyang Wu<sup>c\*</sup>

<sup>a</sup>*School of Food and Biological Engineering, Jiangsu University, Xuefu Rd. 301, Zhenjiang 212013, Jiangsu, China*

<sup>b</sup>*Testing Center, Yangzhou University, Wenhui East Rd. 48, Yangzhou 225009, Jiangsu, China*

<sup>c</sup>*School of the Environment and Safety Engineering, Jiangsu University, Xuefu Rd. 301, Zhenjiang 212013, Jiangsu, China*

<sup>d</sup>*School of Chemistry and Chemical Engineering, Jiangsu University, Xuefu Rd. 301, Zhenjiang 212013, Jiangsu, China*

\*Corresponding author: Tel.:+86 511 88791800; Fax: +86 511 88791800; E-mail address: yangliuqing@ujs.edu.cn (L.-q. Yang).

\*Corresponding author: Tel.:+86 511 88791200; Fax: +86 511 88791200; E-mail address: wuxy@ujs.edu.cn (X.-y. Wu).

<sup>1</sup>Contributed to this article equally and co-first authors.

**Abstract**

The structural characterization, antioxidant activity and protective effect against H<sub>2</sub>O<sub>2</sub>-induced injury RAW264.7 cells of a new polysaccharide (MP1) isolated from *Lepidium meyenii* Walp. were investigated. The molecular weight was estimated to be  $4.67 \times 10^5$  Da by HPLC-ELSD analysis. Monosaccharide composition was determined to be arabinose and galactose in a molar ratio of 2: 1 by GC-MS and PMP-HPLC-UV analysis. Methylation combined with 1D and 2D NMR spectrum analysis revealed that MP1 was an arabinogalactan. MP1 possessed a moderate antioxidant activity *in vitro* in DPPH, ABTS, superoxide and hydroxyl radicals scavenging, Fe<sup>2+</sup> chelating, lipid peroxidation inhibition and reducing power assays. MP1 could also effectively protect RAW264.7 cells from H<sub>2</sub>O<sub>2</sub>-induced injury by maintaining stable cell viability, decreasing ROS, MDA and LDH level and enhancing SOD, GSH-Px and CAT activity. These results suggested the potential utilization of MP1 as a natural antioxidant for food and pharmaceutical applications.

**Key words:** *Lepidium meyenii* Walp.; Polysaccharide; Structure characterization; NMR; Antioxidant activity

## 1. Introduction

*Lepidium meyenii* Walp. (Maca) belonging to the Brassicaceae is a perennial herbaceous plant native to South America, it grows under low temperature and high altitude varying between 3700 and 4450 m [1]. Maca, as a food source, possesses high nutritive value and is rich in starches, proteins, minerals and sugars. Modern pharmacological research showed that maca had many pharmacological activities simultaneously, such as antifatigue, anti-inflammation, enhancing fertility, antioxidative, antiosteoporosis and antidepressant [2-6]. Polysaccharide, macaenes, macamides, alkaloid, flavonolignans and glucosinolates had been identified as major active ingredients [7-10]. Studies on the structural characterization and antioxidant activity of polysaccharide obtained from maca roots or leaves have become a hotspot in recent years. Maca polysaccharide was a kind of heteropolysaccharide, mainly consisting of arabinose (Ara), glucose (Glc), galactose (Gal) and manose (Man) with different molar ratio, the molecular weights ranged from  $6 \times 10^3$  to  $1.1 \times 10^6$  Da, and the glycosyl patterns of maca polysaccharide were T- $\alpha$ -Glc, 1, 3- $\alpha$ -Glc, 1, 3- $\beta$ -Glc, 1, 4- $\alpha$ -Glc, 1, 6- $\alpha$ -Glc, 1, 4, 6- $\alpha$ -Glc, T- $\beta$ -Ara, 1, 5- $\alpha$ -Ara, T- $\alpha$ -Man, 1, 3- $\alpha$ -Man, 1, 2, 6- $\alpha$ -Man, 1, 3- $\beta$ -GalpA and 1, 6- $\beta$ -Gal [5, 6, 11-13]. The antioxidant activities of maca polysaccharides were evaluated based on *in vitro* assays, such as the DPPH assay, superoxide radical assay, hydroxyl radical assay, reducing power assay and ferric-reducing antioxidant power assay. The *in vivo* experiments were carried out on forced swimming mice model and alcoholic liver oxidative injury mice model [13-17]. Maca polysaccharide structure characterization was mainly focused on molecular

weight, glycosyl pattern and monosaccharide composition, but a few studies have been reported on the maca polysaccharides glycosyl sequence. Antioxidant property of polysaccharides produced by maca was determined by several chemical based antioxidant activity assays which do not necessarily reflect the cellular physiological conditions, bioavailability and metabolism. Experiments with animal models are extremely expensive, time-consuming and inappropriate for initial antioxidant screening of food materials. Excess reactive oxygen species (ROS) will lead to oxidative damage to biomacromolecules and finally damage organ function. The process is especially obvious in the immune cells, which exert their biological functions by free radicals and sustain senescent deterioration that related to oxygen stress [18, 19]. The antioxidant activity of maca purified polysaccharide against oxidative stress-induced immune cell injury has not been reported.

In view of the above, a purified polysaccharide (MP1) was obtained from *Lepidium meyenii* Walp., the complete structural information of MP1 was fully explored by GC-MS and NMR analysis including  $^1\text{H}$ ,  $^{13}\text{C}$ , heteronuclear single-quantum coherence (HSQC) experiments, double quantum filtered correlated spectroscopy (DQF-COSY) and heteronuclear multiple-bond correlation (HMBC). DPPH, ABTS, superoxide and hydroxyl radicals scavenging,  $\text{Fe}^{2+}$  chelating, lipid peroxidation inhibition and reducing power assays were used to evaluate the antioxidant activities of the polysaccharide, its protective effects against  $\text{H}_2\text{O}_2$ -induced injury RAW264.7 cells were also evaluated.

## 2. Materials and methods

### 2.1. Materials and chemicals

Maca dry roots were purchased from Wenshan yuanrentang (Wenshan, China). T-series dextrans (T10, T40, T70, T500, T2000) were purchased from Pharmacia Biotechnology Co. (Uppsala, Sweden). Sephacryl™ S-500, DEAE-52, reactive oxygen species (ROS), malonaldehyde (MDA), lactate dehydrogenase (LDH), catalase (CAT), superoxide dismutase (SOD) and glutathione peroxidase (GSH-Px) assay kits were purchased from Hefei Bomei Biotechnology CO. (Hefei, China). 3-(4,5-dimethylthiazol-2-yl)-2,5-diphenyl tetrazolium bromide (MTT), mannose (Man), rhamnose (Rha), galactose (Gal), arabinose (Ara) and glucose (Glc) were purchased from Sigma Chemical Co. (Saint Louis, USA). RAW264.7 cells were purchased from Shanghai Institute of Cell Biology (Shanghai, China) and cultured in DMEM medium supplemented with 10% fetal bovine serum, 100 g/mL streptomycin and 100 IU/mL penicillin at 37 °C in 5% CO<sub>2</sub>.

## 2.2. Isolation and purification of polysaccharide

Maca powder (100 g) was extracted with deionized water (1:20, w/v) for 4 h at 100 °C three times. After centrifugation, the supernatant was concentrated to 400 mL.  $\alpha$ -amylase and glucoamylase were added to the concentrated solution to remove starch. After centrifugation, ethanol was added to the supernatant to a final concentration of 80% (v/v), and kept at 4 °C overnight. The precipitate was collected by centrifugation and dissolved in deionized water, ethanol was removed by vacuum rotary evaporation, the aqueous solution was then collected and deproteinated by trichloroacetic acid (TCA), followed by dialysis and freeze-dried to obtain the crude maca polysaccharide (MP). MP was loaded on a DEAE-52 cellulose column, the column was eluted with deionized

water and then with stepwise gradient of NaCl aqueous solutions (0.05-0.2 M) at a flow rate of 1 mL/min. The major NaCl-eluted fraction was further purified by Sephacryl™ S-500 column, the column was eluted with 0.15 M NaCl at a flow rate of 0.3 mL/min. The main purified polysaccharide fraction was obtained (MP1).

### 2.3. Structure characterization of polysaccharide

#### 2.3.1. HPLC-ELSD analysis

The average molecular weight of MP1 was determined on Agilent HPLC system (Agilent, USA) equipped with an evaporative light scattering detector (ELSD). PL aquagel-OH MIXED-H column (8  $\mu$ m, 7.5  $\times$  300 mm, Agilent, USA) was applied as a separation column. The drift tube temperature was set at 60 °C with the nitrogen flow rate of 1.2 mL/min. The column was eluted with deionized water at a flow rate of 1 mL/min and calibrated with standard dextrans (T10, T40, T70, T500, T2000, Pharmacia, Sweden).

#### 2.3.2. GC-MS analysis

GC-MS analysis was carried out according to the reported method with modification [20, 21], 5 mg MP1 was hydrolyzed with 3 mL H<sub>2</sub>SO<sub>4</sub> (3 M) at 110 °C for 8 h and neutralized with BaCO<sub>3</sub>, the supernatant was lyophilized. Each standard monosaccharides or the hydrolyzed polysaccharide sample with inositol as the internal standard were reacted with hydroxylamine hydrochloride (5 mg), acetic anhydride (0.5 mL) and pyridine (0.5 mL) at 90 °C for 1 h. The aldonitrile acetates derivatives were analyzed with GC-MS (6890N/5975B GC-MS, Agilent, USA).

#### 2.3.3. PMP-HPLC-UV analysis

The PMP-HPLC-UV analysis was carried out as described previously [22]. Each standard monosaccharides or the hydrolyzed polysaccharide sample solution (200  $\mu$ L) was mixed with 0.3 M NaOH (100  $\mu$ L) and 0.5 M 1-Phenyl-3-methyl-5-pyrazalone (PMP)-methanol solution (100  $\mu$ L), the mixture was reacted at 70 °C for 30 min, then neutralized by 0.3 M HCl (100  $\mu$ L). The neutral solution was extracted with CH<sub>3</sub>Cl and the aqueous layer was used for HPLC analysis. All pre-column derivation products were analyzed on Agilent HPLC system (Agilent, USA) with a SHIMADZU VP-ODS column (4.6  $\times$  250 mm, 5  $\mu$ m, Shimadzu, Japan), equipped with an ultraviolet (UV) detector. The column was eluted with ammonium acetate solution (50 mM), and acetonitrile (83:17, v/v) at a flow rate of 1 mL/min.

#### 2.3.4. Methylation analysis

Methylation analysis was performed following previous research [23]. The fully methylated polysaccharide was hydrolyzed with formic acid and trifluoroacetic acid (TFA), followed by reduction with NaBD<sub>4</sub> and acetylation with acetic anhydride to obtain partially methylated alditol acetates (PMAA). The linkage analysis was detected by GC-MS (6890N/5975B GC-MS, Agilent, USA).

#### 2.3.5. NMR analysis

MP1 was dissolved in deuterium oxide (D<sub>2</sub>O) (35 mg/mL), and deuterium-exchanged by freeze-drying thrice from D<sub>2</sub>O. NMR spectra (<sup>1</sup>H, <sup>13</sup>C, HSQC, DQF-COSY, HMBC) were obtained on a Bruker Avance 600 MHz spectrometer (Bruker, Germany) at 60 °C.

#### 2.3.6. Atomic force microscopy (AFM) analysis

The molecular architecture of MP1 was determined by AFM. MP1 solution (100 µg/mL, 5 µL) was dropped onto a freshly cleaved mica surface and allowed to dry at room temperature. AFM was executed on a MFP-3D instrument with tapping-mode (Asylum Research, USA).

#### 2.3.7. Congo red analysis

MP1 was dissolved with Congo red solution (80 µM), followed by the drop-wise addition of 1 M NaOH to 0-0.5 M final concentrations. The visible absorption spectra of MP1 mixture were performed on a UV-2450 Ultraviolet-visible (UV-vis) spectrophotometer (Shimadzu, Japan) at 400-800 nm.

#### 2.4. Antioxidant activity of polysaccharide

##### 2.4.1. Antioxidant activity evaluated by chemical antioxidant assays

##### 2.4.1.1. DPPH radical scavenging assay

The DPPH assay was performed following Xie *et al.* [24]. Briefly, 200 µL of DPPH-ethanol solution (0.1 mM) was added to 100 µL of MP1 polysaccharide solution with different concentrations (0-1000 µg/mL). The mixture maintained at 37 °C for 30 min. The absorbance of the test mixture was tested at 517 nm, ascorbic acid (Vc) was used as reference material, the sample solution was substituted with ethanol as blank control. The scavenging activity of the DPPH radical was calculated as:

$$\text{Scavenging rate (\%)} = [(A_{\text{control}} - A_{\text{sample}}) / A_{\text{control}}] \times 100$$

##### 2.4.1.2. ABTS radical scavenging assay

ABTS assay was performed following Yuan *et al.* [25]. Potassium persulfate (2.45 mM) and ABTS (7 mM) were mixed and incubation at 25 °C for 16 h. The mixture

solution was diluted with deionized water to an absorbance of  $0.70 \pm 0.02$  at 734 nm. 50  $\mu\text{L}$  of MP1 solution (0-1000  $\mu\text{g}/\text{mL}$ ) was added to 100  $\mu\text{L}$  of ABTS solution. After reaction at 25  $^{\circ}\text{C}$  for 6 min, the absorbance was measured at 734 nm, Vc was used as reference material, the sample was replaced with deionized water as blank control. The ABTS scavenging effect was calculated as:

$$\text{Scavenging rate (\%)} = [(A_{\text{control}} - A_{\text{sample}}) / A_{\text{control}}] \times 100$$

#### 2.4.1.3. Superoxide radical scavenging assay

Superoxide radical assay was performed according the method described by Xie *et al.* with modification [26]. 4.5 mL of Tris-HCl buffer (50 mM, pH 8.2) was mixed with 1 mL of MP1 solution (0-1000  $\mu\text{g}/\text{mL}$ ). The mixture was incubated at 25  $^{\circ}\text{C}$  for 20 min, then 0.3 mL pyrogallol (0.025 M) was added to the solution, and the mixture was reacted at 25  $^{\circ}\text{C}$  for 4 min, finally 0.5 mL HCl was added to stop reaction, the absorbance was determined at 325 nm, Vc was used as reference material, the sample was substituted with deionized water as blank control. The superoxide scavenging effect was calculated as:

$$\text{Scavenging rate (\%)} = [(A_{\text{control}} - A_{\text{sample}}) / A_{\text{control}}] \times 100$$

#### 2.4.1.4. Hydroxyl radicals scavenging assay

The hydroxyl radicals scavenging assay was performed following Gao *et al.* [27]. 1 mL of MP1 solution (0-1000  $\mu\text{g}/\text{mL}$ ) was mixed with 3.0 mL of 1, 10-phenanthroline (0.75 mM), 4.0 mL of phosphate buffer (0.2 M, pH 7.4), and 1.0 mL of  $\text{FeSO}_4$  (0.75 mM). Then, 1.0 mL  $\text{H}_2\text{O}_2$  (0.01%, v/v) was added and the mixture was incubated at 37  $^{\circ}\text{C}$  for 1 h, and then the absorbance was measured at 536 nm. Vc was used as reference

material, the sample was substituted with deionized water as blank control. The hydroxyl scavenging effect was calculated as:

$$\text{Scavenging rate(\%)} = [(A_1 - A_0)/(A_2 - A_0)] \times 100$$

where  $A_0$ ,  $A_1$  and  $A_2$  are the absorbances of the blank, sample and control solution (deionized water instead of  $\text{H}_2\text{O}_2$  and sample), respectively.

#### 2.4.1.5. $\text{Fe}^{2+}$ chelating assay

The  $\text{Fe}^{2+}$  assay was performed following Shi *et al.* [28]. Briefly, 220  $\mu\text{L}$  of MP1 solution (0-1000  $\mu\text{g}/\text{mL}$ ) was mixed with 5  $\mu\text{L}$  of  $\text{FeCl}_2$  (2 mM) and then 10  $\mu\text{L}$  of ferrozine (5 mM), shook throughfully and left standing at 25  $^\circ\text{C}$  for 10 min. The absorbance was determined at 562 nm, EDTA-2Na was used as reference material, the sample was substituted with deionized water as blank control. The chelating activity was calculated as:

$$\text{Chelating activity (\%)} = [(A_{\text{control}} - A_{\text{sample}}) / A_{\text{control}}] \times 100$$

#### 2.4.1.6. Lipid peroxidation inhibition assay

According to the method of Ma *et al.* [29], 1 mL of MP1 solution (0-1000  $\mu\text{g}/\text{mL}$ ) was mixed with 0.8 mL yolk suspension, 0.4 mL of  $\text{FeSO}_4$  (25 mM), and incubated at 37  $^\circ\text{C}$  for 60 min. After the addition of 1.0 mL of the 20% TCA and 1.0 mL of TBA, the tubes were placed in a boiling water bath for 15 min, followed by centrifugation, the absorbance of supernatants was then measured at 532 nm, Vc was used as reference material, the sample was replaced with deionized water as blank control. The inhibition of lipid peroxidation was calculated as:

$$\text{Inhibition (\%)} = [(A_{\text{control}} - A_{\text{sample}}) / A_{\text{control}}] \times 100$$

#### 2.4.1.7. Reducing power assay

The  $\text{Fe}^{2+}$  assay was performed following Wang *et al.* [30]. Briefly, 1 mL MP1 solution (0-1000  $\mu\text{g}/\text{mL}$ ) was mixed with 2.5 mL of phosphate buffer (0.2 M, pH 6.6), and 2.5 mL  $\text{K}_3\text{Fe}(\text{CN})_6$  (1%, w/v), the mixture was reacted at 50 °C for 20 min, then cooled to room temperature, 2.5 mL TCA (10%, w/v) was added to stop reaction, followed by centrifugation, 2.5 mL supernatants was mixed with 2.5 mL deionized water and 0.5 mL  $\text{FeCl}_3$  (0.1%, w/v), the mixture was stand at 25 °C for 10 min, then the absorbance was measured at 700 nm. Vc was used as reference material, the sample was replaced with deionized water as blank control. The higher the absorbance, the better was the reducing power.

#### 2.4.2. Antioxidant activity evaluated by $\text{H}_2\text{O}_2$ -induced injury cell model

##### 2.4.2.1. Analysis of cell viability by MTT assay

RAW264.7 cells were seeded in cell culture 96-well plates with density of  $1 \times 10^5$  cells/mL and cultivated for 24 h. Afterwards, the medium was removed, and the new cell medium containing  $\text{H}_2\text{O}_2$  (0.05-4 mM) was added to cultivate for 0.5, 1, 2, 4 h for screening the appropriate  $\text{H}_2\text{O}_2$  concentration and time in the injury model. The group treated by the same cell medium without  $\text{H}_2\text{O}_2$  was taken as control group. To assess the cytoprotection of MP1 on  $\text{H}_2\text{O}_2$ -induced injury cell model, RAW264.7 cells were treated with polysaccharide before  $\text{H}_2\text{O}_2$  was added, the polysaccharide group was treated with MP1 (0-1000  $\mu\text{g}/\text{mL}$ ) and cultivated for 24 h. Afterwards, the medium was removed, new medium containing 1 mM  $\text{H}_2\text{O}_2$  was added to  $\text{H}_2\text{O}_2$  group and polysaccharide group and cultivated for another 1 h. The result was expressed as the cell

viability by MTT assay. The following formula was used:

$$\text{Cell viability (\%)} = \frac{\text{OD value of experimental group}}{\text{OD value of control group}} \times 100\%.$$

#### 2.4.2.2. Determination of ROS

ROS secretion by RAW264.7 cells was tested using 2, 7-dichlorofluorescein diacetate (DCFH-DA). RAW264.7 cells ( $1 \times 10^5$  cells/well, 100  $\mu\text{L}$ /well) were seeded in 96-well plate and incubated for 24 h. Afterwards, the medium was removed, the control group and  $\text{H}_2\text{O}_2$  group was normally cultivated, the polysaccharide group was treated with MP1 (0-1000  $\mu\text{g}/\text{mL}$ ) and cultivated for 24 h. Afterwards, the medium was removed, new medium containing 1  $\text{mM}$   $\text{H}_2\text{O}_2$  was added to  $\text{H}_2\text{O}_2$  group and polysaccharide group and cultivated for another 1 h. Culture medium was carefully removed, followed by the addition of 100  $\mu\text{L}$  of DCFH-DA (10  $\mu\text{M}$ ) for 30 min. Fluorescence intensity was measured on a microplate reader (BioTek, USA) at 520 nm for emission and 485 nm for excitation.

#### 2.4.2.3. Determination of MDA, SOD, GSH-PX, CAT and LDH

RAW264.7 cells ( $1 \times 10^6$  cells/well, 1  $\text{mL}$ /well) were cultivated in 6-well plates under the conditions mentioned above. The level of GSH-Px, SOD, MDA, CAT and LDH in cells were determined by commercial assay kits.

#### 2.5. Statistical analysis

All data are presented as the mean  $\pm$  standard deviation (SD). One-way analysis of variance (ANOVA) and the Tukey method were used for statistical analysis. Significant differences were set at  $P < 0.05$  and  $P < 0.01$ .

### 3. Results and discussion

#### 3.1. Isolation and purification of MP1

The yield of MP was 6.32% of the raw material. MP was then separated and fractionated on DEAE-52 and Sephacryl<sup>TM</sup> S-500 column, one major purified polysaccharide fraction was collected as MP1 (Supplementary Fig. S1). The total carbohydrate of MP1 was 91.7%.

*Figure S1 goes here*

#### 3.2. Structure characterization of MP1

##### 3.2.1. Molecular weight

The HPLC-ELSD profile of MP1 is shown in Supplementary Fig. S2, a single and symmetrical peak indicated the homogeneity of MP1. The retention time of MP1, T10 (10 kDa), T40 (40 kDa), T70 (70 kDa), T500 (500 kDa) and T2000 (2000 kDa) was 7.993, 12.193, 10.842, 9.685, 8.097 and 6.402 min, respectively. According to the standard curve ( $y = -4.7617x + 7.1133$ ,  $R^2 = 0.9903$ ) originated from the retention times of different standard dextrans, the estimated average molecular weight of MP1 was  $4.67 \times 10^5$  Da. Zhang *et al.* obtained a maca purified root polysaccharide MP-1 by DEAE-52 cellulose column with molecular weight of 1067.3 kDa [16]. Two maca purified root polysaccharides MPS-1 and MPS-2 were extracted by water and purified using DEAE-52 and Sephadex G-100 column. The molecular weights of MPS-1 and MPS-2 were 7.6 kDa and 6.7 kDa respectively [17]. The different molecular weights of maca purified root polysaccharides were observed which possibly due to the differences in raw materials and purification methods.

*Figure S2 goes here*

### 3.2.2. Monosaccharide composition

As shown in Fig. 1A, five standard monosaccharides were separated successfully within 20 min. The peaks were identified in the order of Rha, Ara, Man, Glc and Gal by comparing the retention time of the each standard monosaccharide and mass spectrum under the same conditions. As presented in Fig. 1B-D, peaks of MP1 were identified by comparison with the retention time of standard monosaccharides (Fig. 1A) and analysis of mass spectra (Fig. 1 C, D). Accordingly, MP1 was a heteropolysaccharide with arabinose and galactose in a ratio of 2: 1. However, the derivative method used in GC-MS analysis was not suitable for the detection of uronide-containing polysaccharides because uronic acids had the unusual resistance to acid hydrolysis, and decarboxylation and lactonization would occur when uronic acids were liberated from the polymer [31]. Therefore, PMP derivatization was carried out to qualitatively determine the uronic acid and accurately confirm the result of GC-MS analysis. As shown in Fig. 1E, seven PMP-labelled monosaccharides were separated successfully within 36 min. The peaks were identified in the order of Man, Rha, GlcA, GalA, Glc, Gal and Ara by comparing the retention time of the unknown peaks with that of the standards under the same conditions. The calibration curves were calculated by the analysis of six points in the range of 10-200 ug/mL of standard sugars (mannose  $y = 16004x + 173218$   $R^2 = 0.9964$ ; rhamnose  $y = 12611x - 8564$   $R^2 = 0.9995$ ; glucuronic acid  $y = 11922x - 64207$   $R^2 = 0.9993$ ; galacturonic acid  $y = 12488x + 20057$   $R^2 = 0.9988$ ; glucose  $y = 12267x - 1864$   $R^2 = 0.9993$ ; galactose  $y = 16887x + 3919$   $R^2 =$

0.9998; arabinose  $y = 20539x - 39570$   $R^2 = 0.9995$ ). Accordingly, MP1 was a heteropolysaccharide with arabinose and galactose in a ratio of 1.97: 1.00 (Fig. 1F), which was in good agreement with the result of GC-MS analysis. Maca polysaccharides were major composed of Ara, Glc, Gal and Man, for example maca roots polysaccharide MC-1 was composed of Gal (8.32%), Glc (53.66%), Ara (26.21%) and Man (11.81%) [13]. Tang *et al.* revealed that maca root polysaccharide MP contained GalA, Glc, Ara, Man, Gal, Rha in the ratio of 35.07:29.98:16.98:13.01:4.21:0.75 [6]. Ara and gal were major monosaccharide composition in MP1.

*Figure 1 goes here*

### 3.2.3. Methylation analysis

The individual peaks of PMAA were identified according to standard PMAA spectra patterns (Complex Carbohydrate Research Center, University of Georgia, USA), retention time, and combined with literature values [13]. The total ion chromatogram and mass chromatogram of each residue were shown in Fig. 2, and the main fragments for PMAAs were listed in Table 1. GC-MS was performed to indicate the presence of five glycosidic linkages T-Araf, 1, 3-Araf, 1, 5-Araf, 1, 4-Galp and 1, 2, 3, 5-Araf at a molar ratio of 1.8: 2.0: 1.0: 2.5: 1.1. The molar ratios of these residues agreed with the monosaccharide composition in MP1. The molar ratio between branching point and terminal units was 1.2, which was consistent with the fact that the number of terminal units approximately equals to the number of branching points. At present, there are references to report the linkage patterns of maca polysaccharide. Polysaccharide MC-1 had a chain consisting of 1, 5-Araf, 1, 3-Manp, 1, 2, 6-Manp, T-Glcp, 1, 4-Glcp, 1,

6-Glcp and 1, 6-Galp residues [13]. LMP-1 was composed of T-Araf, T-Glcp, 1, 3-Glcp, 1, 4-Glcp, 1, 6-Glcp, and 1, 4, 6-Glcp [12]. The glycosidic linkages were different from MP1.

*Figure 2 goes here*

*Table 1 goes here*

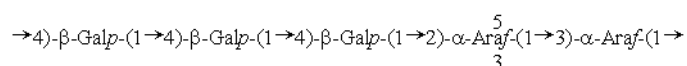
#### 3.2.4. NMR analysis

The NMR spectra were calibrated by D<sub>2</sub>O and the chemical shift of D<sub>2</sub>O was 4.69 ppm (Fig. 3A). The anomeric protons signals at 5.33, 5.26, 5.24, 5.17 and 4.72 ppm were observed in <sup>1</sup>H spectrum (Fig. 3A), which were assigned to residues of A, B, C, D and E, respectively. In the <sup>13</sup>C NMR spectrum (Fig. 3B), anomeric carbon signals occurred at 107.09, 106.59, 106.53, 106.01 and 103.94 ppm. The cross-peaks of 5.33/106.01, 5.26/106.53, 5.24/106.59, 5.17/107.09 and 4.72/103.94 ppm were observed in HSQC spectrum (Fig. 3C).

Residues A, B, C and D were assigned to be  $\alpha$ -arabinofuranose due to characteristic deshielded anomeric carbon signals at 106.01, 106.53, 106.59 and 107.09 ppm. For furanose residue, the chemical shift of anomeric carbon will move to low field at 105-110 ppm in glycosidic linkage [32, 33]. The proton signals for H-2 to H-5 were assigned according to DQF-COSY spectrum (Fig. 3D), and the carbon atoms chemical shifts were readily obtained from the HSQC spectrum (Fig. 3C). The low field position of the C-2 to C-4 carbon resonances in residues A, B, C and D also indicated a five-membered ring furanose configuration [34]. The downfield shifts of residue A C-3 (83.61 ppm), B C-2 (86.61 ppm), B C-3 (83.50 ppm) and B C-5 (65.96 ppm), and C C-5

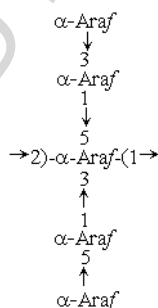
(65.75 ppm) carbon signals indicated that residues A, B and C were 1, 3- $\alpha$ -Araf, 1, 2, 3, 5- $\alpha$ -Araf and 1, 5- $\alpha$ -Araf, respectively [35-37]. To residue D, the downfield shift of C-1 with reference to the standard value, indicating that residue D was substituted at C-1. Residue D was identified as a T- $\alpha$ -Araf [37]. Residue E had anomeric signals at 4.72/103.94 ppm which indicated the presence of  $\beta$ -linked moiety [37]. The chemical shift of C-4 was 76.17 ppm, which suggested the linkage as 1, 4- $\beta$ -Galp of residue E [37, 38]. The completely assigned spectrum of the MP1 is shown in Table 2.

Long-range  $^{13}\text{C}$ - $^1\text{H}$  correlations obtained from the HMBC experiment (Fig. 3E) confirmed the glycosyl sequence. The cross peaks of both anomeric protons and carbons of each sugar residue of MP1 were examined, and both hetero-ring and intra-annular correlation were observed in Fig. 3E. For example, cross peak was found between H-1 (4.72 ppm) of residue E and C-4 (76.17 ppm) of residue E, indicating consecutive linkages of 1, 4- $\beta$ -Galp. Cross peaks between C-1 (103.94 ppm) of residue E and H-2 (4.25 ppm) of residue B, H-1 (5.26 ppm) of residue B and C-3 (83.61 ppm) of residue A, C-1 (106.53 ppm) of residue B and H-3 (4.05 ppm) of residue A, H-1 (5.33 ppm) of residue A and C-4 (76.17 ppm) of residue E were observed in the same way, indicating a probable backbone composed of 1, 4- $\beta$ -Galp, 1, 2- $\alpha$ -Araf, and 1, 3- $\alpha$ -Araf, the backbone was established as below:



Cross peak between H-1 (5.17 ppm) of residue D and C-5 (65.75 ppm) of residue C, and C-1 (107.09 ppm) of residue D and H-5 (3.94 ppm) of residue C indicated that terminal arabinofuranose residues were linked to 1, 5- $\alpha$ -Araf through 1, 5-*O*-glycosidic

bonds. Cross peaks between H-1 (5.17 ppm) of residue D and C-3 (83.61 ppm) of residue A, and C-1 (107.09 ppm) of residue D and H-3 (4.05 ppm) of residue A indicated that terminal arabinofuranose residues were linked to 1, 3- $\alpha$ -Araf through 1, 3-*O*-glycosidic bonds. Cross peak between H-1 (5.33 ppm) of residue A and C-5 (65.96 ppm) of residue B, and C-1 (106.01 ppm) of residue A and C-5 (3.87 ppm) of residue B, indicated that 1, 3- $\alpha$ -Araf was linked to 1, 2, 3, 5- $\alpha$ -Araf through 1, 5-*O*-glycosidic bonds. Cross peak between H-1 (5.24 ppm) of residue C and C-3 (83.50 ppm) of residue B indicated that 1, 5- $\alpha$ -Araf were linked to 1, 2, 3, 5- $\alpha$ -Araf through 1, 3-*O*-glycosidic bonds. Therefore, branches might attach to *O*-3 and *O*-5 of 1, 2- $\alpha$ -Araf, and were composed of 1, 3- $\alpha$ -Araf, 1, 5- $\alpha$ -Araf and T- $\alpha$ -Araf, the branches was established as below:



Some intra residue cross peaks were also observed between H-1 of residue A and its own C-2, C-3; H-1 of residue C and its own C-2, C-3; H-1 of residue D and its own C-2, C-3; C-1 of residue D and its own H-2; C-1 of residue E and its own H-2, H-3. Based on methylation and NMR spectra analysis, the possible structural of MP1 is shown in Fig. 3F.

MP contained 1, 3- $\beta$ -GalpA, 1, 3- $\beta$ -Glc<sub>p</sub> and 1, 3- $\alpha$ -Man<sub>p</sub> linked alternately to

form a backbone (5: 4: 1) [6]. LMP-1 was mainly composed of 1, 4- $\alpha$ -D-Glcp, 1, 6- $\alpha$ -D-Glcp, 1, 3- $\alpha$ -D-Glcp, and T- $\beta$ -D-Araf, with branching at O-6 of 1, 4, 6- $\alpha$ -D-Glcp [12]. The structures were different from MP1, possibly due to the differences between the raw materials, isolation methods and purification fraction.

*Figure 3 goes here*

*Table 2 goes here*

### 3.2.5. AFM analysis

AFM has been used as a valuable metrological tool to characterize surface topology of polysaccharides [39]. As shown in Fig. 4A, MP1 had a random twist shape by twisting of each polysaccharide chain. Section analysis showed the height of MP1 ranged from 1 to 3 nm, the height of single polysaccharide chain was about 0.1-1 nm (Fig. 4B), which indicated that MP1 polysaccharide chains entangled with each other and the structure of MP1 was branched. AFM analysis were coincided with the predicted structure of MP1.

### 3.2.6. Congo red analysis

The polysaccharides in a helical conformation can form complexes with Congo red, which will lead to a bathochromic shift of complexes in comparison with pure Congo red. As shown in Fig. 4C, there was no notable shifts in  $\lambda_{\max}$  between Congo red and MP1-Congo red complex with the increasing NaOH concentration. This finding suggested that MP1 existed as random coils instead of triple-helical structure. The result was consistent with the Congo-red tests of other random coils of active polysaccharides [20].

*Figure 4 goes here*

### 3.3. Antioxidant activity of MP1

#### 3.3.1. Antioxidant activity evaluated by chemical antioxidant assays

##### 3.3.1.1. DPPH radical scavenging activity

DPPH assay, an efficient and rapid method, has been widely used to evaluate the free radical scavenging ability of polysaccharide [40]. As shown in Fig. 5A, MP1 exhibited obvious DPPH radical scavenging effect in a dose-dependent manner ranging from 100 to 1000  $\mu\text{g/mL}$ , the scavenging rates of MP1 on DPPH radicals were in the range of 9.12-31.23%, suggesting that MP1 exerted moderate DPPH radical scavenging activity. Compared with four maca roots refined polysaccharides LMPs [14], the DPPH radical scavenging ability of MP1 was greater than LMP-60, LMP-70 and LMP-90, but similar with LMP-80. The difference in scavenging activity may be related to the fact that LMPs were obtained by different concentration of ethanol precipitation.

##### 3.3.1.2. ABTS radical scavenging activity

The total antioxidant ability of MP1 was measured by means of scavenging a protonated radical ABTS [41]. As shown in Fig. 5B, the ABTS radical scavenging activities of MP1 were well-correlated with the concentrations and increased as the concentrations increased. The scavenging effects of MP1 on ABTS increased from 2.56% to 22.35% ranging from 100 to 1000  $\mu\text{g/mL}$ . The results indicated that MP1 had a moderate capacity to scavenge ABTS.

##### 3.3.1.3. Superoxide radical scavenging activity

Superoxide radical is formed from mitochondrial electron transport systems, can

induce lipid peroxidation production and hydroxyl radical, which are harmful for biomolecules (DNA, proteins, and enzymes) [42]. As shown in Fig. 5C, MP1 showed a dose-response relationship, the scavenging effects of MP1 on superoxide radical increased from 10.39% to 22.28% ranging from 100 to 1000  $\mu\text{g/mL}$ . The results indicated that MP1 had a moderate capacity to scavenge superoxide radical.

#### 3.3.1.4. Hydroxyl radicals scavenging activity

Hydroxyl radical can easily cross cell membranes, readily react with most biomolecules (DNA, lipids, proteins, and carbohydrates) and cause tissue damage or cell death [43]. As shown in Fig. 5D, MP1 showed a dose-response relationship, the scavenging effects of MP1 on hydroxyl radical increased from 12.14% to 36.89% ranging from 100 to 1000  $\mu\text{g/mL}$ . Polysaccharide LMP-60 obtained from maca roots exhibited the highest hydroxyl radical scavenging ability (52.9%) at 2.0  $\text{mg/mL}$  [14], which was similar with MP1. The results indicated that MP1 had a moderate capacity to scavenge hydroxyl radical.

Previous studies have indicated that polysaccharides possess a radical scavenging activity are related to the number of available active hydroxyl groups in structure [44-46]. The results suggested that MP1 showed a moderate capacity to scavenge four radicals by either an electron transfer mechanism or a hydrogen atom.

#### 3.3.1.5. $\text{Fe}^{2+}$ chelating activity

Some transition metals can evoke the production of free radicals and aggravate the cellular oxidative damage. Among the transition metals, Fe is an extremely active metal.  $\text{Fe}^{2+}$  will promote lipid oxidation via the Fenton reaction [47]. Thus, it has been

recognized that chelating  $\text{Fe}^{2+}$  may inhibit lipid oxidation. As shown in Fig. 5E, chelating abilities of MP1 increased as their concentrations climbed up. At the concentration of 1000  $\mu\text{g}/\text{mL}$ , the chelating activity of MP1 on  $\text{Fe}^{2+}$  was 49.23%. These results revealed that MP1 demonstrate an effective capacity for  $\text{Fe}^{2+}$  chelating. The  $\text{Fe}^{2+}$  chelating activity was shown dependent on the number of hydroxyl, and the hydroxyl substitution in the ortho position [48].

#### 3.3.1.6. Lipid peroxidation inhibition activity

Lipid peroxidation, an important event in cellular damage, is strongly associated with aging, carcinogenesis and other diseases [49]. As shown in Fig. 5F, lipid peroxidation inhibition activity of MP1 climbed up as their concentrations increased. At the concentration of 1000  $\mu\text{g}/\text{mL}$ , the inhibition activity of MP1 on lipid peroxidation was 58.31%. These results revealed that MP1 demonstrate an effective capacity for lipid peroxidation inhibition. The mechanism of the inhibitory effect of MP1 might involve reducing power and radical scavenging activity [50].

#### 3.3.1.7. Reducing power

The reducing power serves as a significant potential antioxidant index. As shown in Fig. 5G, the reducing power of MP1 correlated well with increasing concentrations. When the MP1 concentration increased from 100 to 1000  $\mu\text{g}/\text{mL}$ , the reducing power of MP1 increased from 0.193 to 0.475. Li *et al.* reported that the reducing power of maca leaves polysaccharides (LMLP) was 0.079 at 1.0  $\text{mg}/\text{mL}$ , which was lower than that of MP1 [51]. The reducing power is usually related to the presence of reducing agents which have been shown to exert antioxidant action by breaking the free radical chain

and giving rise to a hydrogen atom [52].

Monosaccharide composition is one of most influencing factors for the antioxidant activities of polysaccharides, e.g. galactose and arabinose content [53], Li *et al.* reported that arabinose appeared critical in determining EC50 of DPPH-scavenging activity by evaluating quantitative structure activity relationship (QSAR) models for the antioxidant activity of polysaccharides [54]. Arabinose and galactose were the major groups of MP1 monosaccharide composition.

*Figure 5 goes here*

### 3.3.2. Antioxidant activity evaluated by H<sub>2</sub>O<sub>2</sub>-induced injury cell model

#### 3.3.2.1. Cell model and polysaccharide treatment

MTT assay indicated that MP1 has no toxicity on RAW264.7 macrophage cells (data not shown), it had been selected as model cells in the study. H<sub>2</sub>O<sub>2</sub> is a reactive oxygen species (ROS), which may damage cells through direct oxidation on biomolecules (lipids, proteins, DNA), or act as a signaling molecule to trigger intracellular pathways leading to cell death [55]. The results in Fig. 6A show that exposure of RAW264.7 cells to H<sub>2</sub>O<sub>2</sub> induced a concentration dependent and time dependent viability loss in cells. The viability of cells incubated with 1 mM H<sub>2</sub>O<sub>2</sub> for 1 h was 59.59% of the control value. Therefore, in the next experiments, added 1 mM H<sub>2</sub>O<sub>2</sub> to the cells for 1 h to study the effect of MP1 on H<sub>2</sub>O<sub>2</sub>-induced injury RAW264.7 cells.

As shown in Fig. 6B, MP1 exhibited a significant protective effect in a dose-dependent manner against H<sub>2</sub>O<sub>2</sub>-induced injury RAW264.7 cell, when the

concentration increased from 400  $\mu\text{g/mL}$  to 1000  $\mu\text{g/mL}$ , the cells viability of MP1 group was significant improved compared with the  $\text{H}_2\text{O}_2$  model group ( $p < 0.01$ ). The results implied that MP1 observably protected RAW264.7 cells against  $\text{H}_2\text{O}_2$ -induced cytotoxicity.

*Figure 6 goes here*

### 3.3.2.2. Effect of MP1 on the level of ROS in cells

ROS levels are determined based on DCFH-DA fluorescence. When cells are injured by  $\text{H}_2\text{O}_2$ , plenty of ROS (superoxide, hydrogen peroxide, and hydroxyl) will generate to oxidize DCFH into DCF [56]. As shown in Fig. 7, the fluorescence intensity of  $\text{H}_2\text{O}_2$  model group was significantly larger than that of control group ( $P < 0.01$ ). However, pre-treatment with MP1 effectively prevented ROS generation relative to  $\text{H}_2\text{O}_2$ -treated cells and the suppressing effect gradually was strengthened with the increasing concentrations of MP1 ( $P < 0.01$ ). The result suggested that the cytoprotective effects of MP1 may result from inhibition of intracellular ROS production.

*Figure 7 goes here*

### 3.3.2.3. Effect of MP1 on the level of MDA, LDH, SOD, GSH-PX and CAT in cells

Oxidative cellular damage caused by ROS is normally along with an increase in lipid peroxide, which will decrease enzyme activity and membrane fluidity [57]. MDA is the major secondary metabolite of lipid peroxidation [58]. LDH release is usually used as an indicator for cell membranes integrity [59]. As shown in Fig. 8A, B, the released MDA and LDH significant increased in model group, all of which was

statistical significant as compared with control group ( $P < 0.01$ ), indicating that  $H_2O_2$  produce cell damage. The level of MDA and LDH released by the polysaccharide group were lower than those of model group, indicating the oxidative damage level of cells decreased due to MP1 protection. When at 1000  $\mu\text{g/mL}$ , MP1 showed superlative protection ability, the amount of MDA was significantly ( $P < 0.01$ ) decreased to 2.19 nmol/mg prot compared with that of model group (4.08 nmol/mg prot), and LDH significantly ( $P < 0.01$ ) reduced to 507.41 U/L compared with that of the model group (1026.75 U/L). SOD, GSH-Px and CAT are important free radical scavenging enzymes and in the first line of defense against oxidative injury. The status of these antioxidant enzymes is an appropriate indirect way to assess the pro-oxidant-antioxidant status in tissues [60]. SOD plays an important role in the defense against ROS [61], GSH-Px is another important antioxidant enzyme for engine body to eliminate superoxide anion [58], CAT can eliminate hydrogen peroxide [62], they serve as an important protective system to prevent damage caused by ROS. As shown in Fig. 8C-E, when compared with the control group, cells treated with  $H_2O_2$  alone showed acute damage as evidenced by a significant decline in SOD, GSH-Px and CAT in  $H_2O_2$  injured RAW264.7 cells ( $P < 0.01$ ). Interestingly, preincubation of cells with MP1 markedly promoted elevations in the levels of SOD ( $P < 0.01$ ) and GSH-Px ( $P < 0.01$ ) at 200  $\mu\text{g/mL}$ , and CAT ( $P < 0.01$ ) at 400  $\mu\text{g/mL}$  as compared with cells treated with  $H_2O_2$  alone. Maca root polysaccharide MP-1 also dramatically increased the SOD and GSH-Px levels in alcoholic mice at a dose of 200, 600, 1800 mg/kg [16]. Polysaccharide MPS-1 and MPS-2 from maca root could significantly reduce the level of LDH in forced swimming mice at a dose of 100

mg/kg [17]. Maca root polysaccharide MP treatment could significantly enhance GSH-Px, and reduce the levels of LDH and MDA at a dose of 100 mg/kg [6]. All those results indicate that inhibition of lipid peroxides and enhancing antioxidant enzyme activity might be involved in the protective effects of MP1 in RAW264.7 cells. .

In previous reports, a selenium polysaccharide (PGP1) from *Platycodon grandiflorum* could rescue PC12 cell death caused by H<sub>2</sub>O<sub>2</sub> via inhibiting oxidative stress, PGP1 could inhibit the decrease of cell viability, decrease the apoptotic rates, prevent membrane damage (LDH release), attenuate intracellular ROS formation, increase SOD activity and decreased MDA in PC12 cells after H<sub>2</sub>O<sub>2</sub> exposure [63]. Liu *et al.* reported that *Rheum tanguticum* polysaccharide could preserve over 90% of intestinal epithelial cell survival after H<sub>2</sub>O<sub>2</sub> insult and decrease LDH leakage and cell apoptosis at 300 µg/mL [64]. Therefore, some bioactive polysaccharides can improve the viability of cell to reduce H<sub>2</sub>O<sub>2</sub>-induced apoptosis and necrosis. MP1 was a kind of water-soluble neutral polysaccharide, the structure feature may contribute to the protective effect against H<sub>2</sub>O<sub>2</sub>-induced injury RAW264.7 cells.

*Figure 8 goes here*

#### 4. Conclusion

Polysaccharide MP1 was isolated from maca, the structural study demonstrated that MP1 was an arabinogalactan. MP1 exhibited a moderate capacity for scavenging the DPPH, ABTS, superoxide and hydroxyl radicals, chelating activity of Fe<sup>2+</sup>, inhibition of lipid peroxidation, and reducing power. MP1 also exhibited significant protective effect on H<sub>2</sub>O<sub>2</sub>-injured RAW264.7 cells. Therefore, it is recommended that

MP1 could be explored as a potential natural antioxidant. The further structure-activity relationships would be investigated in the future.

### Acknowledgments

The authors are grateful for the financial support by Science and Technology Plan of Zhenjiang (GY2012002) and Graduate Innovative Projects in Jiangsu Province (KYLX 1073).

### Reference

- [1] Y. Wang, Y. Wang, B. Mcneil, L. M. Harvey, Maca: An Andean crop with multi-pharmacological functions, *Food. Res. Int.* 40 (2007) 783-792.
- [2] K. Yoshida, Y. Ohta, N. Kawate, M. Takahashi, T. Inaba, S. Hatoya, H. Morii, K. Takahashi, M. Ito, H. Tamada, Long-term feeding of hydroalcoholic extract powder of *Lepidium meyenii* (maca) enhances the steroidogenic ability of Leydig cells to alleviate its decline with ageing in male rats, *Andrologia.* 50 (2017) e12803.
- [3] K. S. Gugnani, N. Vu, A. N. Rondónortiz, M. Böhlke, T. J. Maher, A. J. Pinofigueroa, Neuroprotective activity of macamides on manganese-induced mitochondrial disruption in U-87 MG glioblastoma cells, *Toxicol. Appl. Pharm.* 340 (2018) 67-76.
- [4] B. Tenci, C. M. L. Di, M. Maresca, L. Micheli, G. Pieraccini, N. Mulinacci, C. Ghelardini, Effects of a water extract of *Lepidium meyenii* root in different models of persistent pain in rats, *Z. Natureforsch. C.* 72 (2017) 449-457.
- [5] M. M. Zhang, W. J. Wu, R. Yao, X. F. Li, Y. Q. Tang, M. Tian, F. Lai, W. Hui, Structural characterization of a novel polysaccharide from *Lepidium meyenii* (maca) and analysis of its regulatory function in macrophage polarization in vitro, *J. Agric. Food. Chem.* 65 (2017) 1146-1157.
- [6] W. M. Tang, L. Jin, L. H. Xie, J. Q. Huang, N. Wang, B. Q. Chu, X. L. Dai, Y. Liu, R. Wang, Y. Zhang, Structural characterization and antifatigue effect in vivo of

- maca (*Lepidium meyenii* Walp.) polysaccharide, *J. Food. Sci.* 82 (2017) 757-764.
- [7] M. Zhou, R. Q. Zhang, Y. J. Chen, L. M. Liao, Y. Q. Sun, Z. H. Ma, Q. F. Yang, P. Li, Y. Q. Ye, Q. F. Hu, Three new pyrrole alkaloids from the roots of *Lepidium meyenii*, *Phytochem. Lett.* 23 (2018) 137-140.
- [8] L. Z. Lin, J. Y. Huang, D. X. Sun-Waterhouse, M. M. Zhao, K. Zhao, J. J. Que, Maca (*Lepidium meyenii*) as a source of macamides and polysaccharide in combating of oxidative stress and damage in human erythrocytes, *Int. J. Food. Sci. Tech.* 53 (2018) 304-312.
- [9] S. X. Chen, K. K. Li, D. Pubu, S. P. Jiang, B. Chen, L. R. Chen, Z. Yang, C. Ma, X. J. Gong, Optimization of ultrasound-assisted extraction, HPLC and UHPLC-ESI-Q-TOF-MS/MS analysis of main macamides and macaenes from Maca (Cultivars of *Lepidium meyenii* Walp), *Molecules.* 22 (2017) 2196-2211.
- [10] Q. H. Zhang, K. Q. Wu, Y. Xu, S. D. Ding, F. Q. Ye, X. B. Wang, Q. Zhang, K. Wu, Y. Xu, S. Ding, Pharmacokinetics and tissue distribution of N-3-methoxybenzyl-palmitamide in rat: A macamide derived from *Lepidium meyenii*, *Trop. J. Pharm. Res.* 16 (2017) 2039-2046.
- [11] Y. J. Li, F. X. Xu, M. M. Zheng, X. Z. Xi, X. W. Cui, C. C. Han, Maca polysaccharides: A review of compositions, isolation, therapeutics and prospects, *Int. J. Biol. Macromol.* 111 (2018) 894-902.
- [12] Z. Q. Zha, S. Y. Wang, W. H. Chu, Y. Lv, H. J. Kan, Q. L. Chen, L. L. Zhong, L. Yue, J. N. Xiao, Y. Wang, H. P. Yin, Isolation, purification, structural characterization and immunostimulatory activity of water-soluble polysaccharides from *Lepidium meyenii*, *Phytochemistry.* 147 (2018) 184-193.
- [13] M. M. Zhang, G. Wang, F. R. Lai, H. Wu, Structural characterization and immunomodulatory activity of a novel polysaccharide from *Lepidium meyenii*. *J. Agric. Food. Chem.* 64 (2016) 1921-1931.
- [14] S. H. Zha, Q. S. Zhao, J. J. Chen, L. W. Wang, G. F. Zhang, H. Zhang, B. Zhao, Extraction, purification and antioxidant activities of the polysaccharides from maca (*Lepidium meyenii*), *Carbohydr. Polym.* 111 (2014) 584-587.
- [15] C. C. Kang, L. M. Hao, L. M. Zhang, Z. Q. Zheng, Y. W. Yang, Isolation,

- purification and antioxidant activity of polysaccharides from the leaves of maca (*Lepidium Meyenii*), *Int. J. Biol. Macromol.* 107 (2017) 2611-2619.
- [16] L. J. Zhang, Q. S. Zhao, L.W. Wang, M. X. Zhao, B. Zhao, Protective effect of polysaccharide from maca (*Lepidium meyenii*) on Hep-G2 cells and alcoholic liver oxidative injury in mice. *Int. J. Biol. Macromol.* 99 (2017) 63-70.
- [17] J. Li, Q. R. Sun, Q. R. Meng, L. Wang, W. T. Xiong, L. F. Zhang, Anti-fatigue activity of polysaccharide fractions from *Lepidium meyenii* Walp. (maca), *Int. J. Biol. Macromol.* 95 (2017) 1305-1311.
- [18] X. B. Yang, Y. Zhao, Y. Lv, Chemical composition and antioxidant activity of an acidic polysaccharide extracted from *Cucurbita moschata* duchesne ex Poiret, *J. Agr. Food. Chem.* 55 (2007) 4684-4690.
- [19] X. T. Zhang, X. Q. Sun, C. Wu, J. L. Chen, J. J. Yuan, Q. F. Pang, Z. P. Wang, Heme oxygnease-1 induction by methylene blue protects RAW264.7 cells from hydrogen peroxide-induced injury. *Biochem. Pharmacol.* 148 (2018) 265-277.
- [20] Q. Li, W. Wang, Y. Zhu, Y. Chen, W. J. Zhang, P. Yu, G. H. Mao, T. Zhao, W. W. Feng, L. Q. Yang, Structural elucidation and antioxidant activity a novel Se-polysaccharide from Se-enriched *Grifola frondosa*, *Carbohydr. Polym.* 161 (2017) 42-52.
- [21] D. T. Wu, W. Z. Li, J. Chen, Q. X. Zhong, Y. J. Ju, J. Zhao, A. Bzhelyansky, S. P. Li, An evaluation system for characterization of polysaccharides from the fruiting body of *Hericium erinaceus* and identification of its commercial product, *Carbohydr. Polym.* 124 (2015) 201-207.
- [22] X. Yang, Y. Zhao, Q. Wang, H. Wang, Q. Mei, Analysis of the monosaccharide components in Angelica polysaccharides by high performance liquid chromatography, *Anal. Sci.* 21 (2005) 1177-1180.
- [23] T. Zhao, G. H. Mao, W. W. Feng, R. W. Mao, X. Y. Gu, T. Li, Q. Li, Y. T. Bao, L. Q. Yang, X. Y. Wu, Isolation, characterization and antioxidant activity of polysaccharide from *Schisandra sphenanthera*, *Carbohydr. Polym.* 105 (2014) 26-33.
- [24] X. F. Xie, G. L. Zou, C. H. Li, Purification, characterization and in vitro

- antioxidant activities of polysaccharide from *Chaenomeles speciosa*, *Int. J. Biol. Macromol.* 92 (2016) 702-707.
- [25] B. Yuan, X. Q. Yang, M. Kou, C. Y. Lu, Y. Y. Wang, J. Peng, P. Chen, J. H. Jiang, Selenylation of polysaccharide from the sweet potato and evaluation of antioxidant, antitumor, and antidiabetic activities, *J. Agr. Food. Chem.* 65 (2017) 605-617.
- [26] J. H. Xie, Z. J. Wang, M. Y. Shen, S. P. Nie, B. Gong, H. S. Li, Q. Zhao, W. J. Li, M. Y. Xie, Sulfated modification, characterization and antioxidant activities of polysaccharide from *Cyclocarya paliurus*, *Food. Hydrocolloid.* 53 (2016) 7-15.
- [27] J. Gao, T. Zhang, Z. Y. Jin, X. M. Xu, J. H. Wang, X. Q. Zha, H. Q. Chen, Structural characterisation, physicochemical properties and antioxidant activity of polysaccharide from *Lilium lancifolium* Thunb, *Food. Chem.* 169 (2015) 430-438.
- [28] J. J. Shi, J. G. Zhang, Y. H. Sun, J. Qu, L. Li, C. Prasad, Z. J. Wei, Physicochemical properties and antioxidant activities of polysaccharides sequentially extracted from peony seed dreg, *Int. J. Biol. Macromol.* 91 (2016) 23-30.
- [29] L. Ma, H. Chen, W. Zhu, Z. Wang, Effect of different drying methods on physicochemical properties and antioxidant activities of polysaccharides extracted from mushroom *Inonotus obliquus*, *Food. Res. Int.* 50 (2013) 633-640.
- [30] C. C. Wang, S. C. Chang, B. S. Inbaraj, B. H. Chen, Isolation of carotenoids, flavonoids and polysaccharides from *Lycium barbarum* L. and evaluation of antioxidant activity, *Food. Chem.* 120 (2010) 184-192.
- [31] Y. G. Niu, W. Yan, J. L. Lv, W. B. Yao, L. L. Yu, Characterization of a novel polysaccharide from *Tetraploid Gynostemma pentaphyllum* Makino. *J. Agr. Food. Chem.* 61(2013) 4882-4889.
- [32] O. Ahrazem, P. J. A. Leal, Fungal cell wall polysaccharides isolated from *Discula destructiva* spp, *Carbohydr. Res.* 342 (2007) 1138-1143.
- [33] B. Yang, K. N. Prasad, Y. Jiang, Structure identification of a polysaccharide purified from litchi (*Litchi chinensis* Sonn.) pulp, *Carbohydr. Polym.* 137 (2016) 570-575.
- [34] S. Górska, W. Jachymek, J. Rybka, M. Strus, P. B. Heczko, A. Gamian, Structural

- and immunochemical studies of neutral exopolysaccharide produced by *Lactobacillus johnsonii* 142, *Carbohyd. Res.* 345 (2010) 108-114.
- [35] S. M. Cardoso, A. M. S. Silva, M. A. Coimbra, Structural characterisation of the olive pomace pectic polysaccharide arabinan side chains, *Carbohyd. Res.* 337(10) (2002) 917-924.
- [36] D. Hua, D. Zhang, B. Huang, P. Yi, C. Yan, Structural characterization and DPPH· radical scavenging activity of a polysaccharide from Guara fruits, *Carbohyd. Polym.* 103 (2014) 143-147.
- [37] L. Xu, J. Cao, W. Chen, Structural characterization of a broccoli polysaccharide and evaluation of anti-cancer cell proliferation effects, *Carbohyd. Polym.* 126 (2015) 179-184.
- [38] T. Zhao, G. H. Mao, M. Zhang, W. W. Feng, R. W. Mao, Y. Zhu, X. Y. Gu, Q. L. L. Q. Yang, X. Y. Wu, Structure analysis of a bioactive heteropolysaccharide from *Schisandra chinensis* (Turcz.) Baill., *Carbohyd. Polym.* 103 (2014) 488-495.
- [39] Y. F. Wang, Y. H. Peng, X. L. Wei, Z. W. Yang, J. B. Xiao, Z. Y. Jin, Sulfation of tea polysaccharides: synthesis, characterization and hypoglycemic activity, *Int. J. Biol. Macromol.* 46 (2010) 270-274.
- [40] R. Amarowicz, R. B. Pegg, P. Rahimi-Moghaddam, B. Barl, J. A. Weil, Free-radical scavenging capacity and antioxidant activity of selected plant species from the *Canadian prairies*, *Food. Chem.* 84 (2004) 551-562.
- [41] A. X. Luo, X. J. He, S. D. Zhou, Y. J. Fan, A. S. Luo, C. Ze, Purification, composition analysis and antioxidant activity of the polysaccharides from *Dendrobium nobile* Lindl, *Carbohyd. Polym.* 79 (2010) 1014-1019.
- [42] O. Blokhina, E. Virolainen, K. V. Fagerstedt, Antioxidants, oxidative damage and oxygen deprivation stress: a review, *Ann. Bot-london.* 91 (2003) 179-194.
- [43] J. F. Yuan, Z. Q. Zhang, Z. C. Fan, J. X. Yang, Antioxidant effects and cytotoxicity of three purified polysaccharides from *Ligusticum chuanxiong* Hort, *Carbohyd. Polym.* 74 (2008) 822-827.
- [44] M. Shi, Z. Zhang, Y. Yang, Antioxidant and immunoregulatory activity of *Ganoderma lucidum* polysaccharide (GLP), *Carbohyd. Polym.* 95 (2013) 200-206.

- [45] M. Y. Shon, T. H. Kim, N. J. Sung, Antioxidants and free radical scavenging activity of *Phellinus baumii* (Phellinus of Hymenochaetaceae) extracts, Food. Chem. 82 (2003) 593-597.
- [46] J. Macdonald, H. F. Galley, N. R. Webster, Oxidative stress and gene expression in sepsis, Brit. J. Anaesth. 90 (2003) 221-232.
- [47] S. N. El, S. Karakaya, Radical scavenging and iron-chelating activities of some greens used as traditional dishes in Mediterranean diet, Int. J. Food. Sci. Nutr. 55 (2004) 67-74.
- [48] G. C. Yen, P. D. Duh, D. Y. Chuang, Antioxidant activity of anthraquinones and anthrone, Food. Chem. 70 (2000) 437-441.
- [49] H. J. Yang, X. H. Zhang, Polysaccharides from *Polygonatum odoratum* strengthen antioxidant defense system and attenuate lipid peroxidation against exhaustive exercise-induced oxidative stress in mice, Trop. J. Pharm. Res. 16 (2017) 795-801.
- [50] X. Li, A. Zhou, Y. Han, Anti-oxidation and anti-microorganism activities of purification polysaccharide from *Lygodium japonicum* in vitro, Carbohydr. Polym. 66 (2006) 34-42.
- [51] S. F. Li, L. M. Hao, Q. Z. Kang, Y. X. Cui, H. Jiang, X. Liu, J. Lu, Purification, characterization and biological activities of a polysaccharide from *Lepidium meyenii* leaves, Int. J. Biol. Macromol. 103 (2017)1302-1310.
- [52] K. B. Jeddou, F. Chaari, S. Maktouf, O. Nouriellouz, C. B. Helbert, R. E. Ghorbel, Structural, functional, and antioxidant properties of water-soluble polysaccharides from potatoes peels, Food. Chem. 205 (2016) 97-105.
- [53] J. Lu, L. You, Z. Lin, M. Zhao, C. Cui, The antioxidant capacity of polysaccharide from *Laminaria japonica* by citric acid extraction, Int. J. Food. Sci. Tech. 48 (2013) 1352-1358.
- [54] Z. M. Li, K. Y. Nie, Z. J. Wang, D. H. Luo, Quantitative structure activity relationship models for the antioxidant activity of polysaccharides, Plos. One. 11 (2016) e0163536.
- [55] K. M. Holmström, T. Finkel, Cellular mechanisms and physiological consequences of redox-dependent signalling, Nat. Rev. Mol. Cell. Biol. 15 (2014) 411-421.

- [56] C. P. Lebel, H. Ischiropoulos, S. C. Bondy, Evaluation of the probe 2',7'-dichlorofluorescein as an indicator of reactive oxygen species formation and oxidative stress, *Chem. Res. Toxicol.* 5 (1992) 227-231.
- [57] J. E. Park, J. H. Yang, S. J. Yoon, J. H. Lee, E. S. Yang, J. W. Park, Lipid peroxidation-mediated cytotoxicity and DNA damage in U937 cells, *Biochimie.* 84 (2002) 1198-1204.
- [58] X. Xiao, J. Liu, J. Hu, X. Zhu, H. Yang, C. Wang, Y. Zhang, Protective effects of protopine on hydrogen peroxide-induced oxidative injury of PC12 cells via Ca(2+) antagonism and antioxidant mechanisms, *Eur. J. Pharmacol.* 591 (2008) 21-27.
- [59] Z. L. Liu, Q. Liu, B. Xiao, J. Zhou, J. G. Zhang, Y. Li, The vascular protective properties of kinsenoside isolated from *Anoectochilus roxburghii* under high glucose condition, *Fitoterapia.* 86 (2013) 163-170.
- [60] S. M. Sabirac, A. Hamid, M. Q. Khan, M. L. Athayde, D. B. Santos, A. A. Boligon, J. B. T. Rocha, Antioxidant and hepatoprotective activity of ethanolic extract of leaves of *Solidago microglossa* containing polyphenolic compounds, *Food. Chem.* 131 (2012) 741-747.
- [61] W. Tang, M. Y. Shen, J. H. Xie, D. Liu, M. X. Du, L. H. Lin, H. Gao, B. R. Hamaker, M. Y. Xie, Physicochemical characterization, antioxidant activity of polysaccharides from *Mesona chinensis* Benth and their protective effect on injured NCTC-1469 cells induced by H<sub>2</sub>O<sub>2</sub>, *Carbohydr. Polym.* 175(2017) 538-546.
- [62] J. Krychmadej, L. Gebicka, Do pH and flavonoids influence hypochlorous acid-induced catalase inhibition and heme modification?, *Int. J. Biol. Macromol.* 80 (2015) 162-169.
- [63] Y. Sheng, G. Liu, M. Wang, Z. Lv, P. Du, A selenium polysaccharide from *Platycodon grandiflorum* rescues PC12 cell death caused by H<sub>2</sub>O<sub>2</sub> via inhibiting oxidative stress, *Int. J. Biol. Macromol.* 104 (2017) 393-399.
- [64] L. N. Liu, Q. B. Mei, L. Liu, F. Zhang, Z. G. Liu, Z. P. Wang, R. T. Wang, Protective effects of *Rheum tanguticum* polysaccharide against hydrogen peroxide-induced intestinal epithelial cell injury, *World. J. Gastro.* 11 (2005) 1503-1507.

**Figure caption**

**Figure 1** The GC-MS chromatograms of standard monosaccharides (A) and MP1 (B), the mass chromatograms of Ara (C) and Gal (D) in MP1 and the HPLC chromatograms of PMP derivatives of standard monosaccharides (E) and MP1 (F).

**Figure 2** The total ion chromatogram from methylation analysis of MP1 (A), the mass chromatograms of T-Araf (B), 1,3-Araf (C), 1,5-Araf (D), 1,4-Galp (E) and 1,2,3,5-Araf (F) in MP1.

**Figure 3** The  $^1\text{H}$  NMR spectra (A),  $^{13}\text{C}$  NMR spectra (B),  $^1\text{H}/^{13}\text{C}$  HSQC correlation spectra (C),  $^1\text{H}/^1\text{H}$  DQF-COSY correlation spectra (D),  $^1\text{H}/^{13}\text{C}$  HMBC correlation spectra (E) and the predict structure (F) of MP1.

**Figure 4** AFM 2D map (A), AFM section analysis (B) of MP1 and Change trend of maximum absorption wavelength of MP1-Congo red complex (C).

**Figure 5** DPPH radical scavenging activity (A), ABTS radical scavenging activity (B), superoxide radical scavenging activity (C), hydroxyl radicals scavenging activity (D),  $\text{Fe}^{2+}$  chelating activity (E) lipid peroxidation inhibition activity (F) and reducing power (G) of MP1.

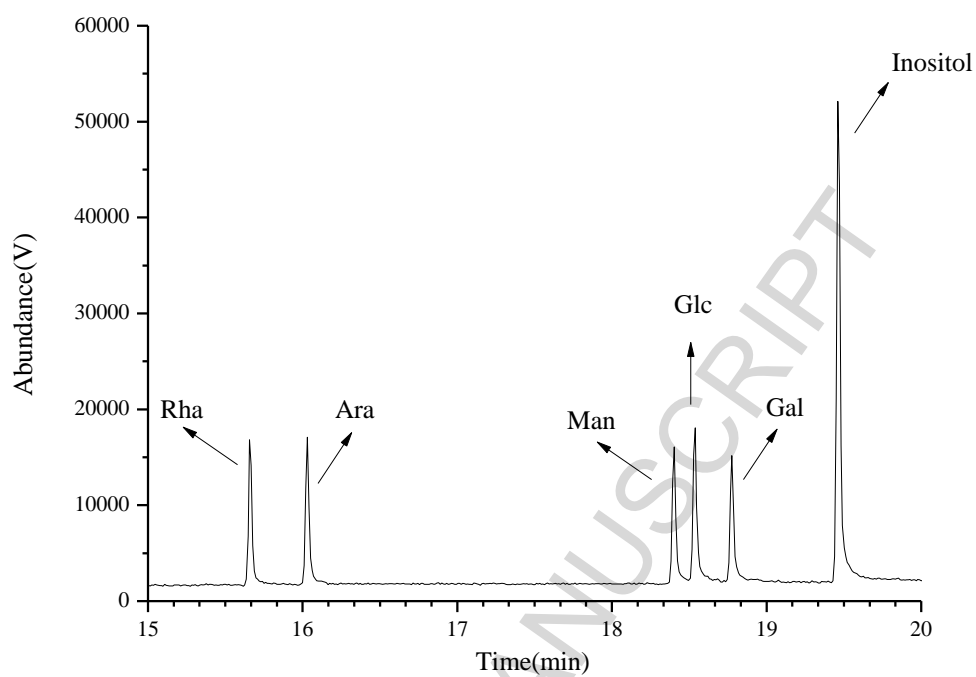
**Figure 6** (A) Effect of  $\text{H}_2\text{O}_2$  on RAW264.7 cells viability; (B) Effect of MP1 on  $\text{H}_2\text{O}_2$ -induced injury RAW264.7 cells viability. Results shown are expressed as means  $\pm$  SD,  $*P < 0.05$ ,  $**P < 0.01$  vs control group,  $^aP < 0.05$ ,  $^{aa}P < 0.01$  vs model group.

**Figure 7** Effect of MP1 on the level of ROS in  $\text{H}_2\text{O}_2$ -induced injury RAW264.7 cells. Results shown are expressed as means  $\pm$  SD,  $*P < 0.05$ ,  $**P < 0.01$  vs control group,  $^aP < 0.05$ ,  $^{aa}P < 0.01$  vs model group.

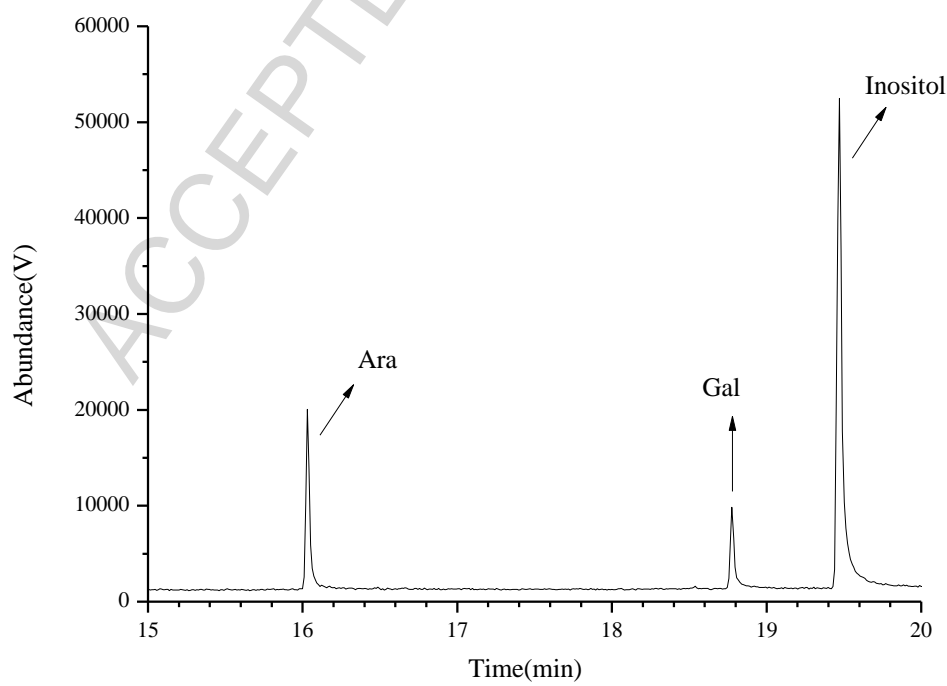
**Figure 8** Effect of MP1 on the level of MDA (A), LDH (B), SOD (C), GSH-Px (D), and CAT (E) in H<sub>2</sub>O<sub>2</sub>-induced injury RAW264.7 cells. Results shown are expressed as means  $\pm$  SD, \**P* < 0.05, \*\**P* < 0.01 vs control group, <sup>a</sup>*P* < 0.05, <sup>aa</sup>*P* < 0.01 vs model group.

ACCEPTED MANUSCRIPT

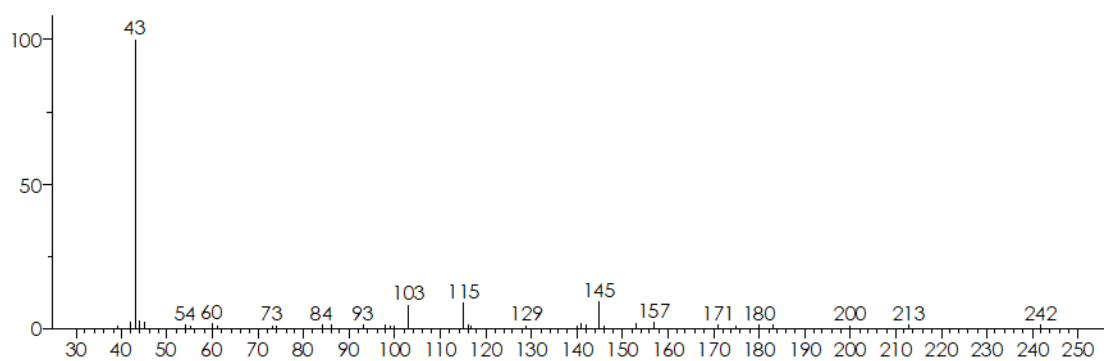
Figure 1



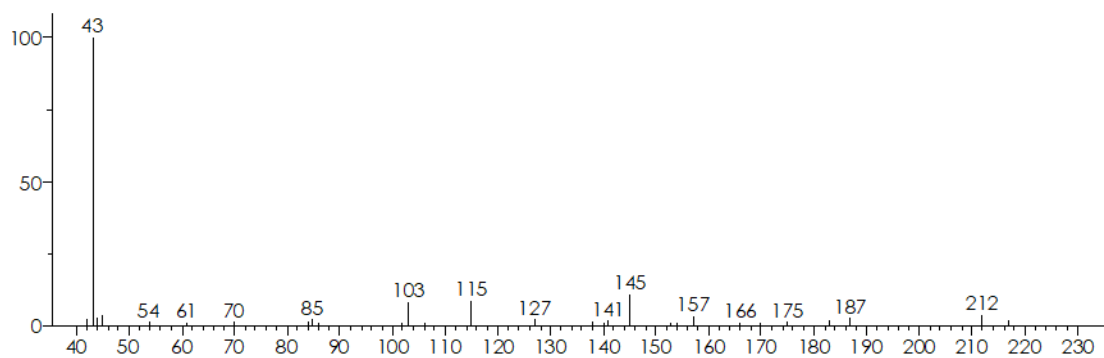
(A)



(B)

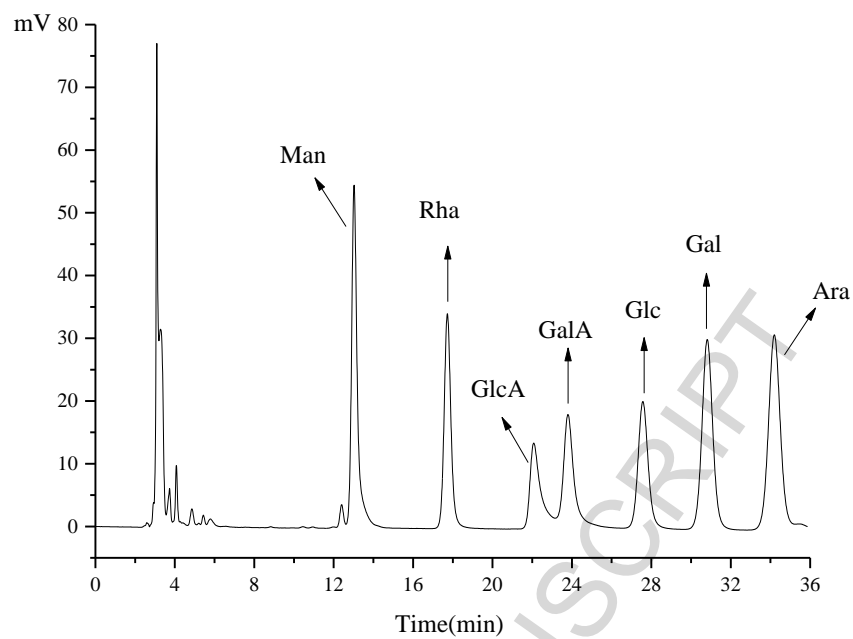


(C)

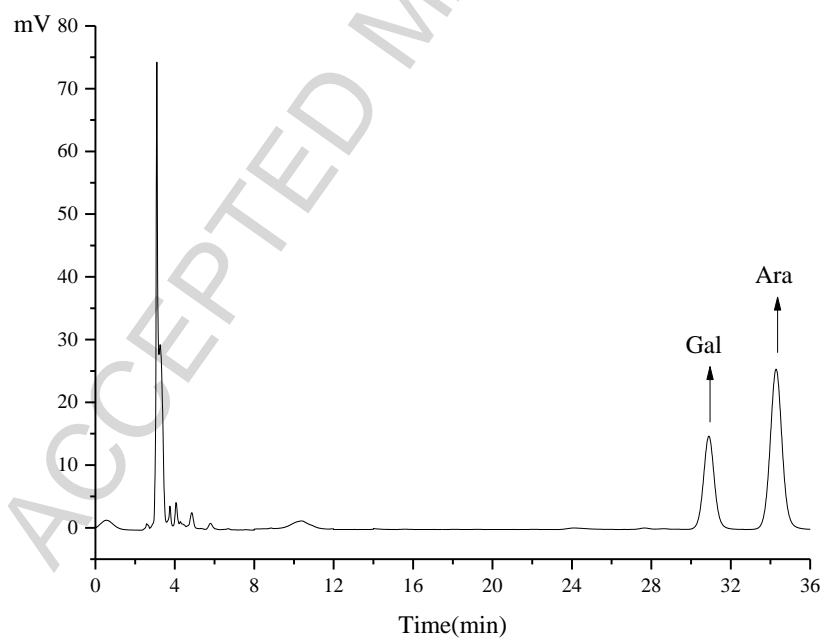


(D)

ACCEPTED

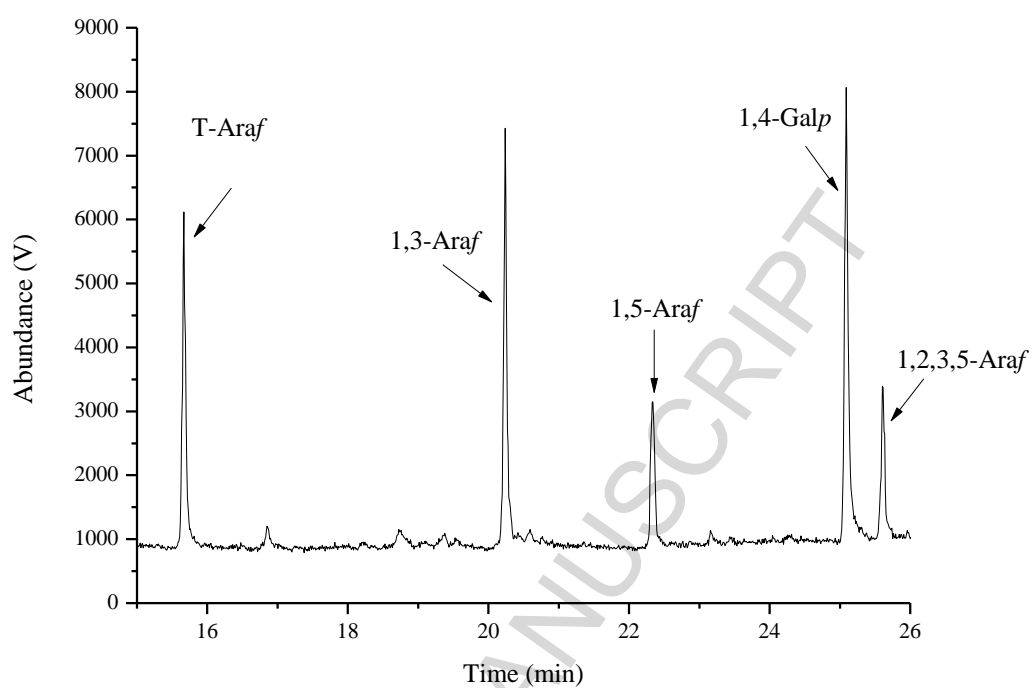


(E)

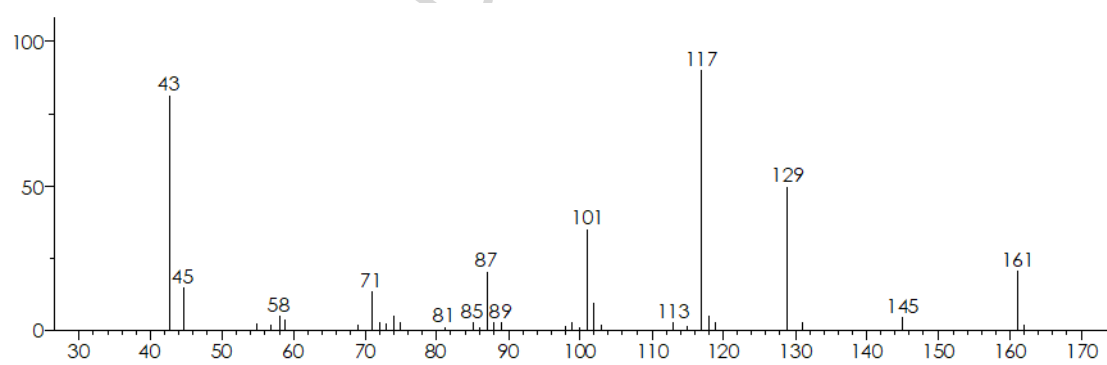


(F)

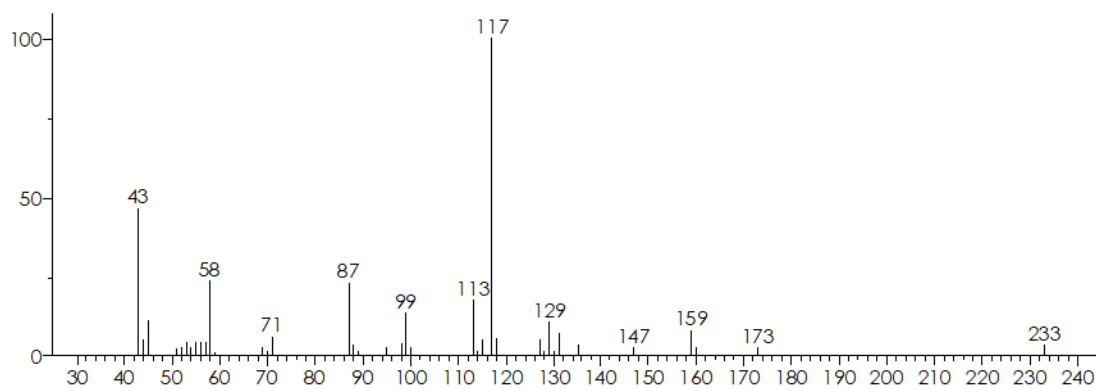
Figure 2



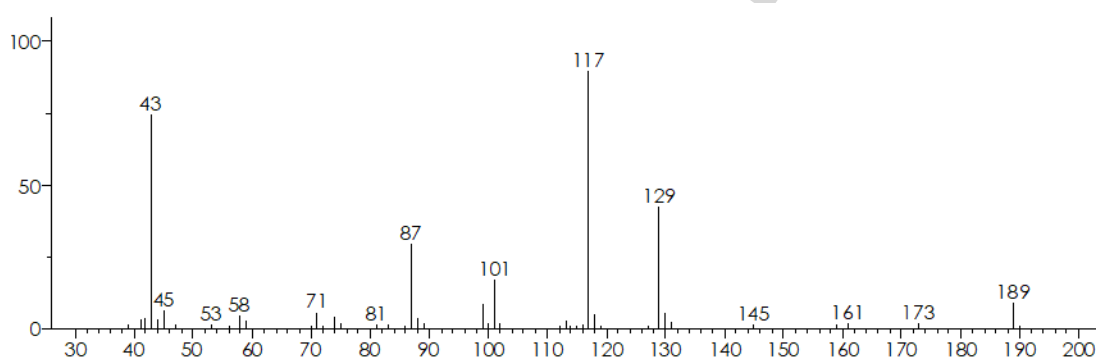
(A)



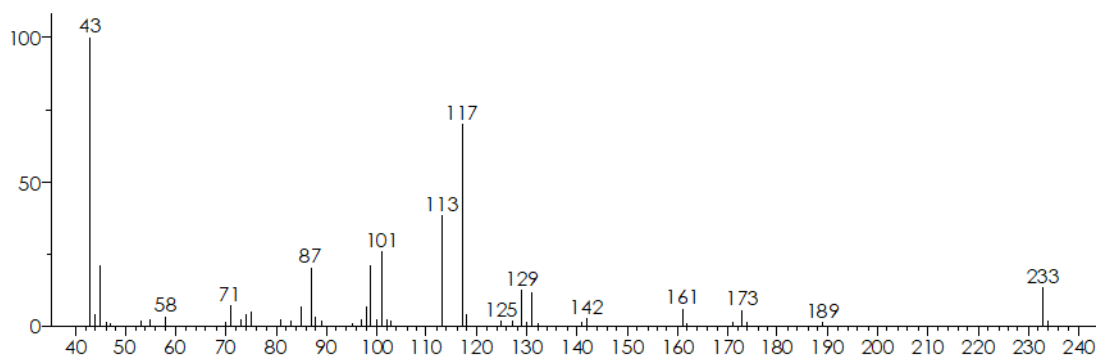
(B)



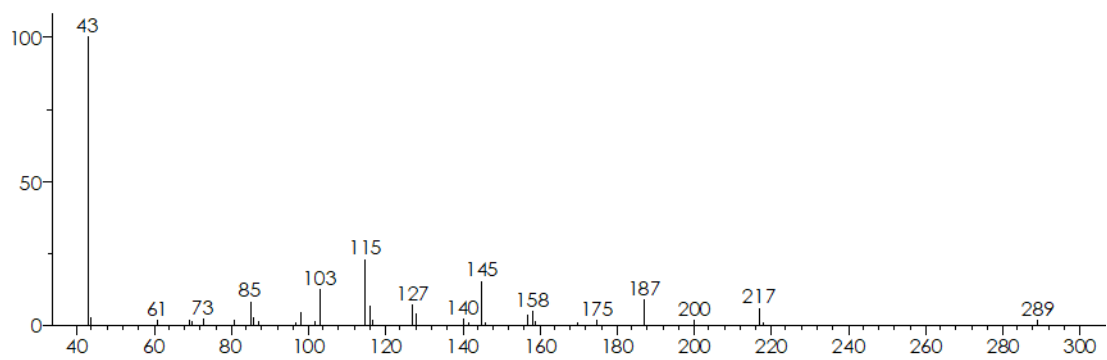
(C)



(D)



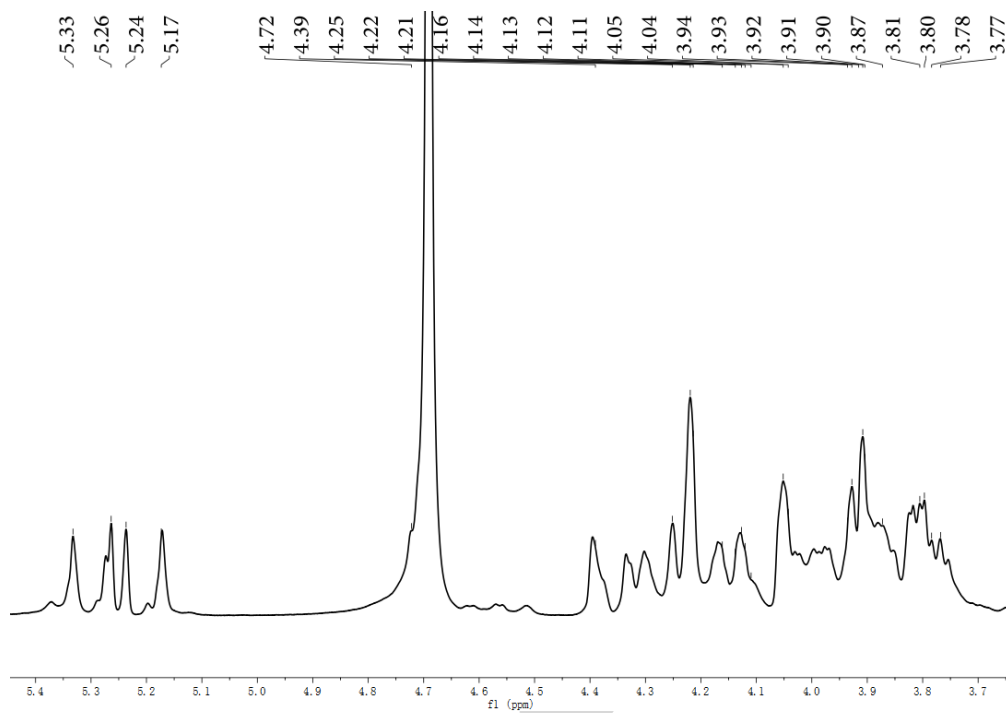
(E)



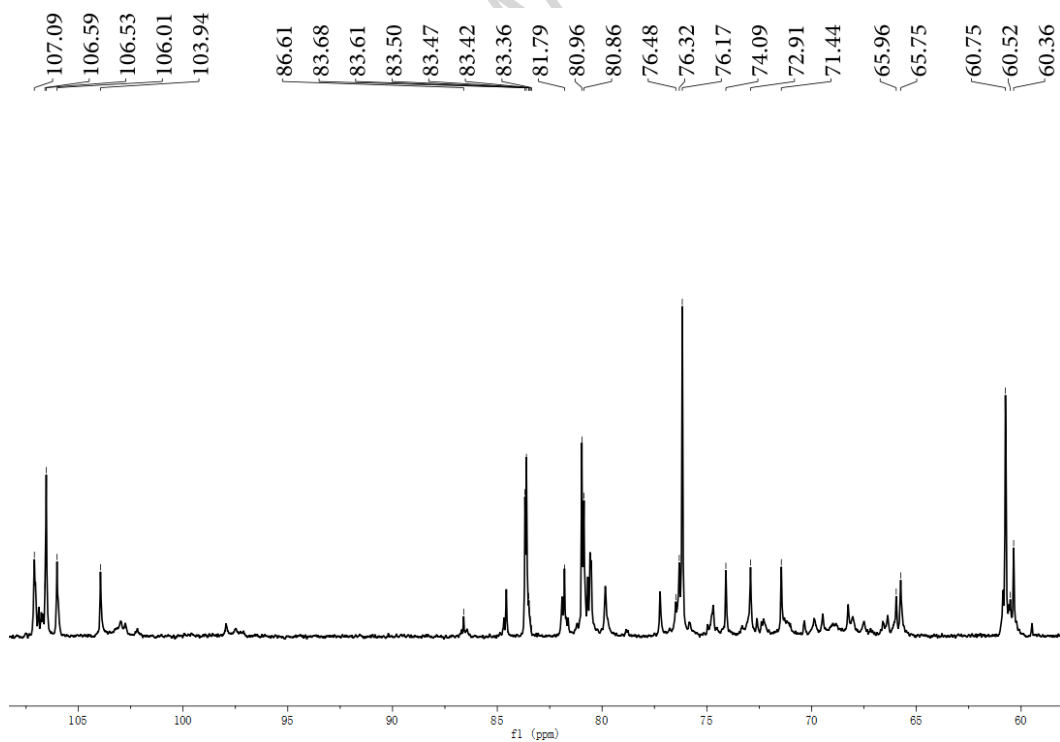
(F)

ACCEPTED MANUSCRIPT

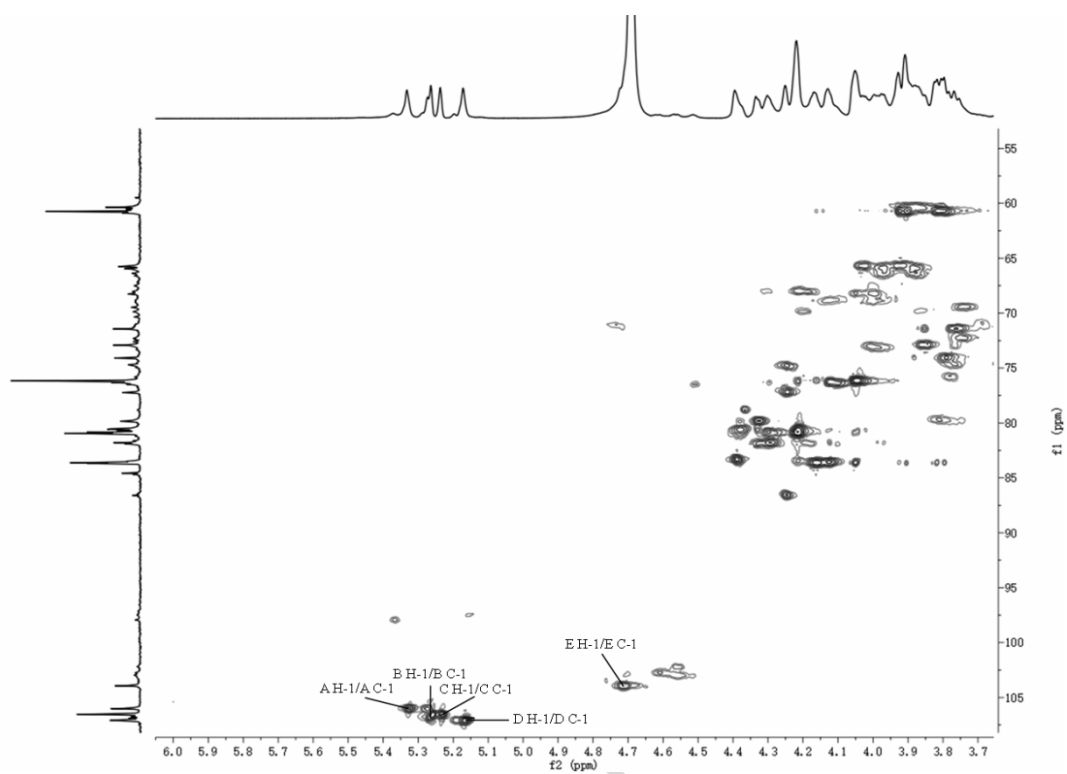
Figure 3



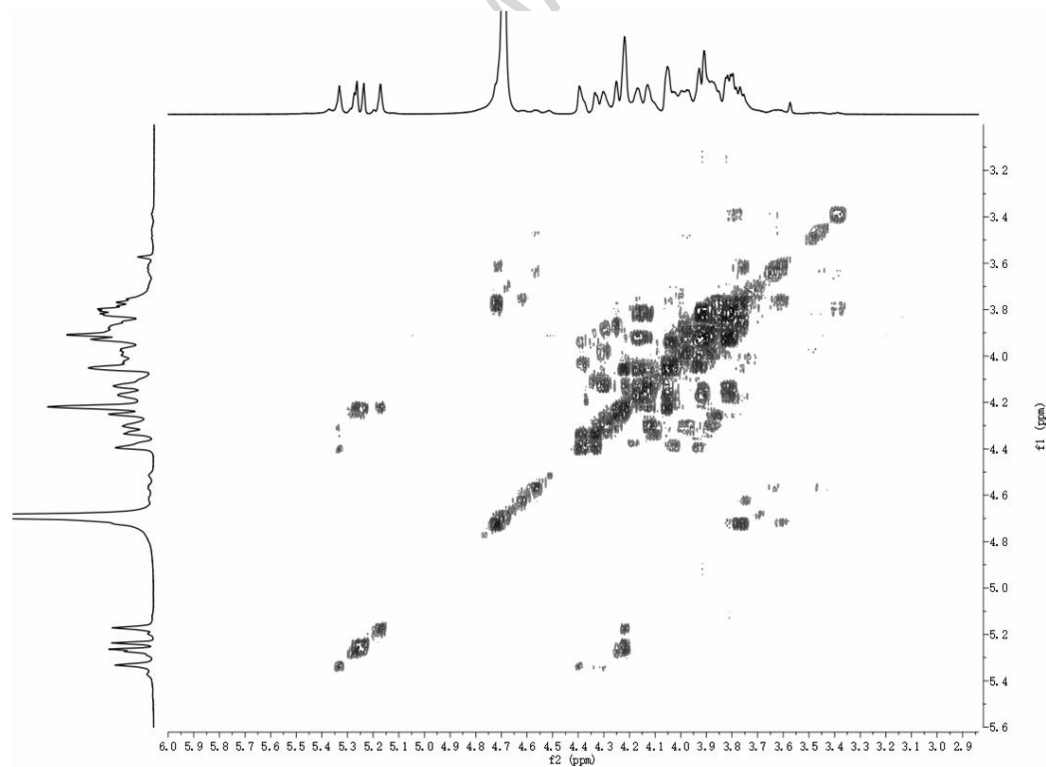
(A)



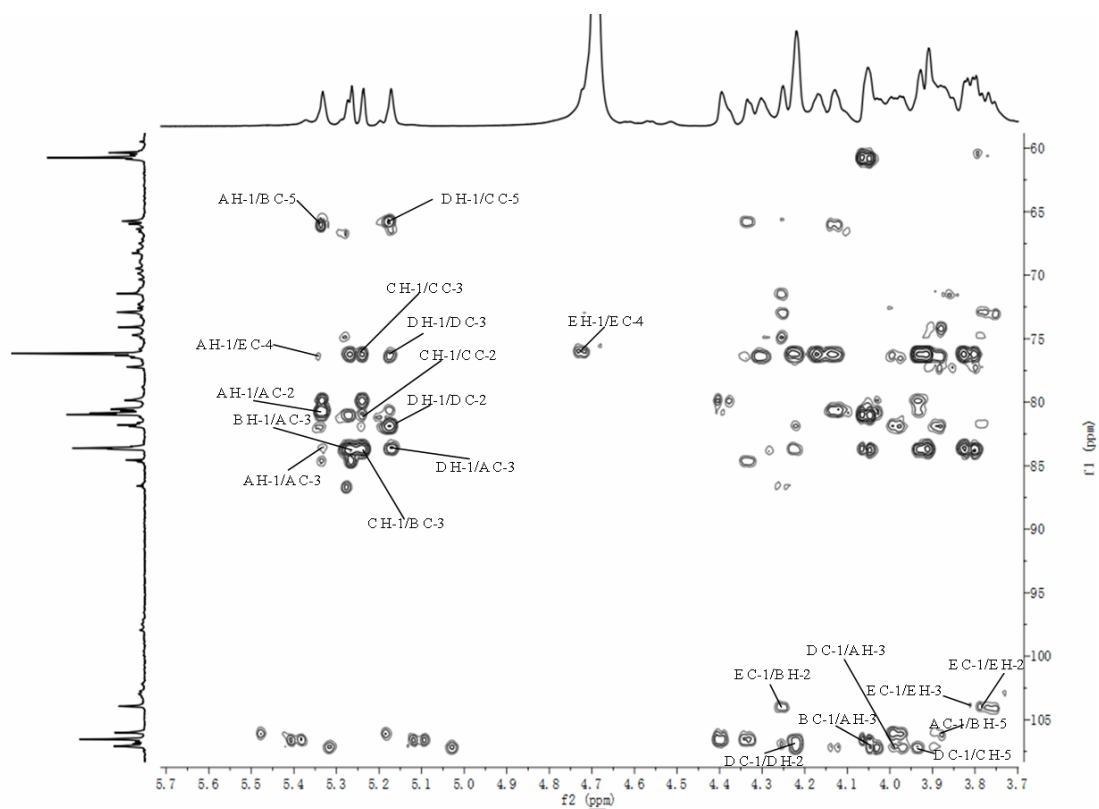
(B)



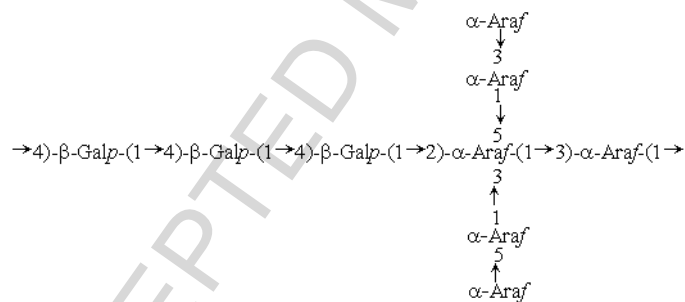
(C)



(D)

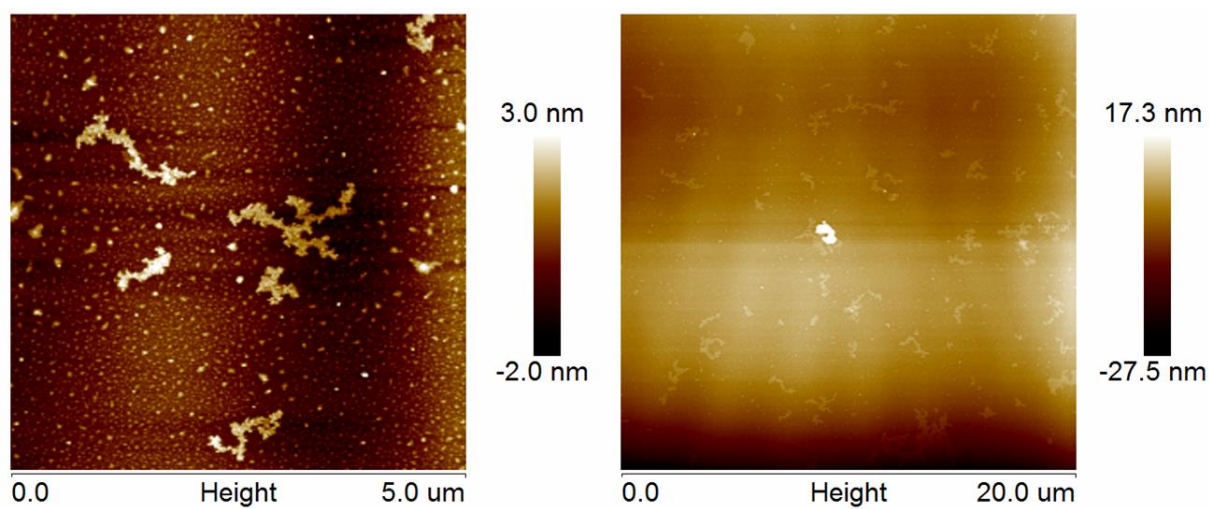


(E)



(F)

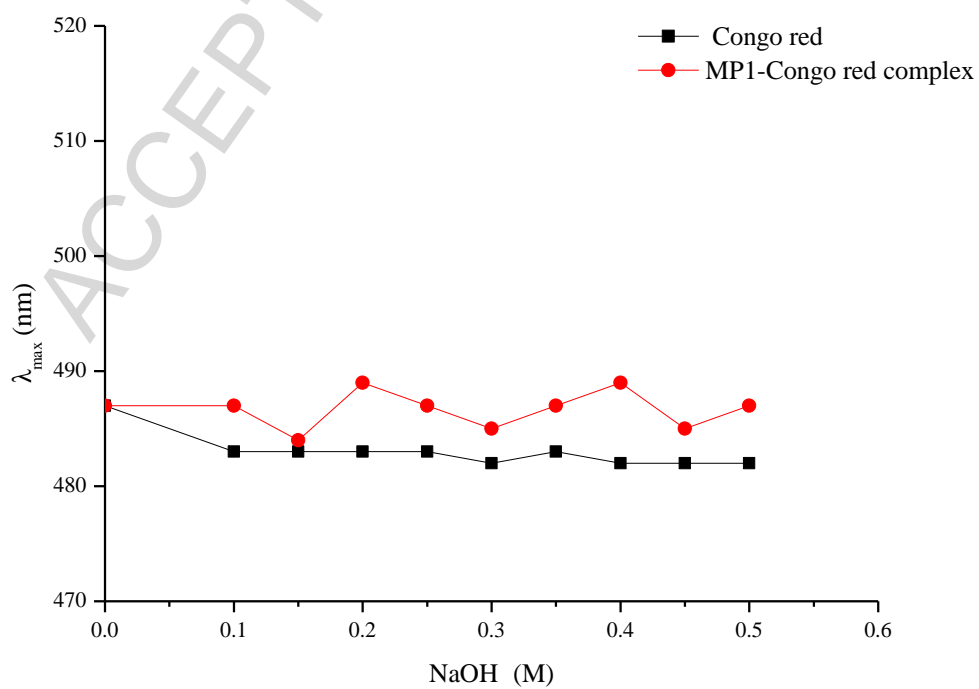
Figure 4



(A)



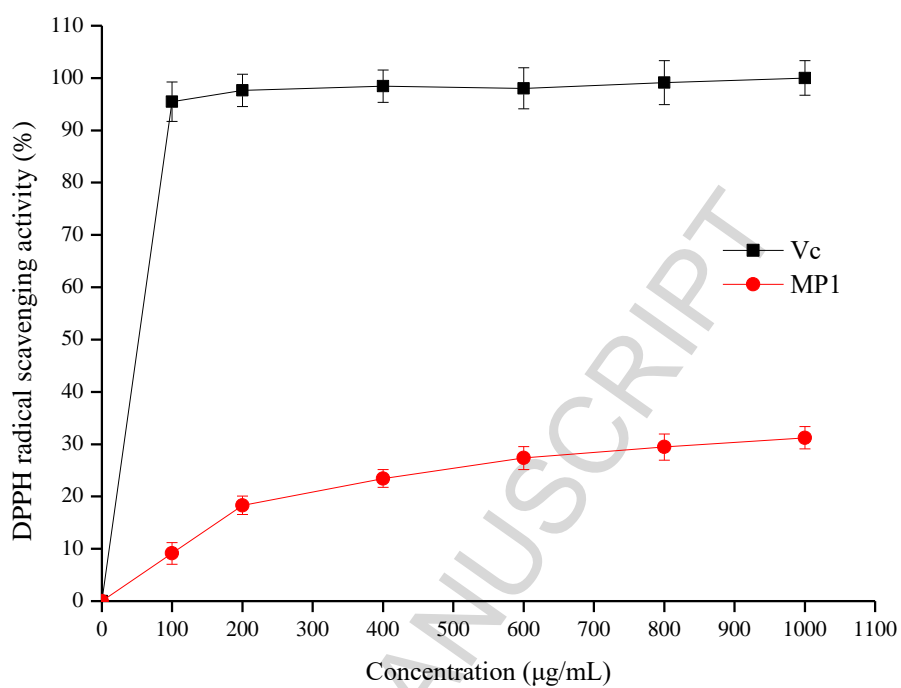
(B)



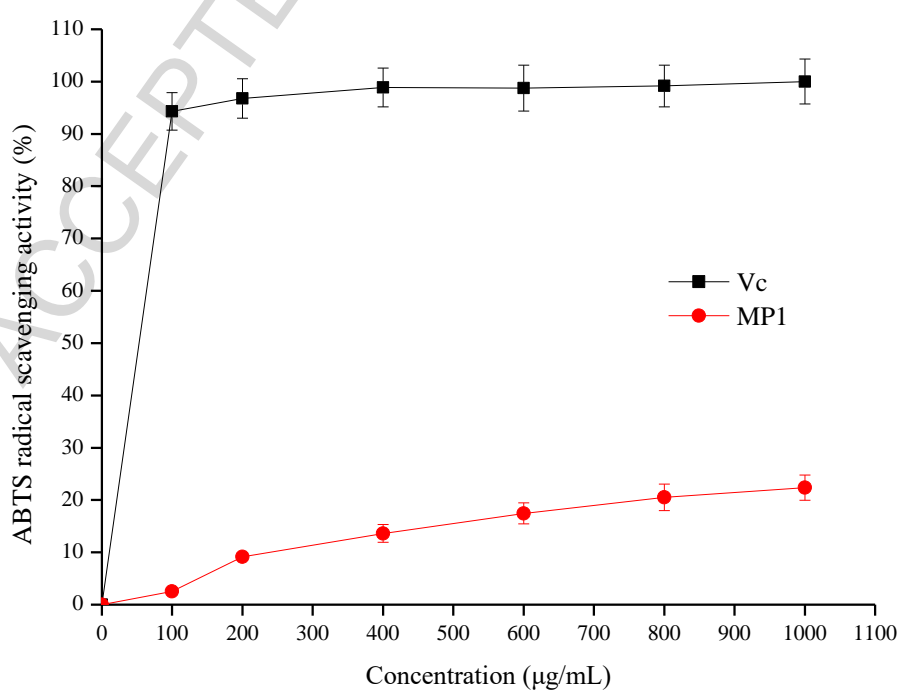
(C)

ACCEPTED MANUSCRIPT

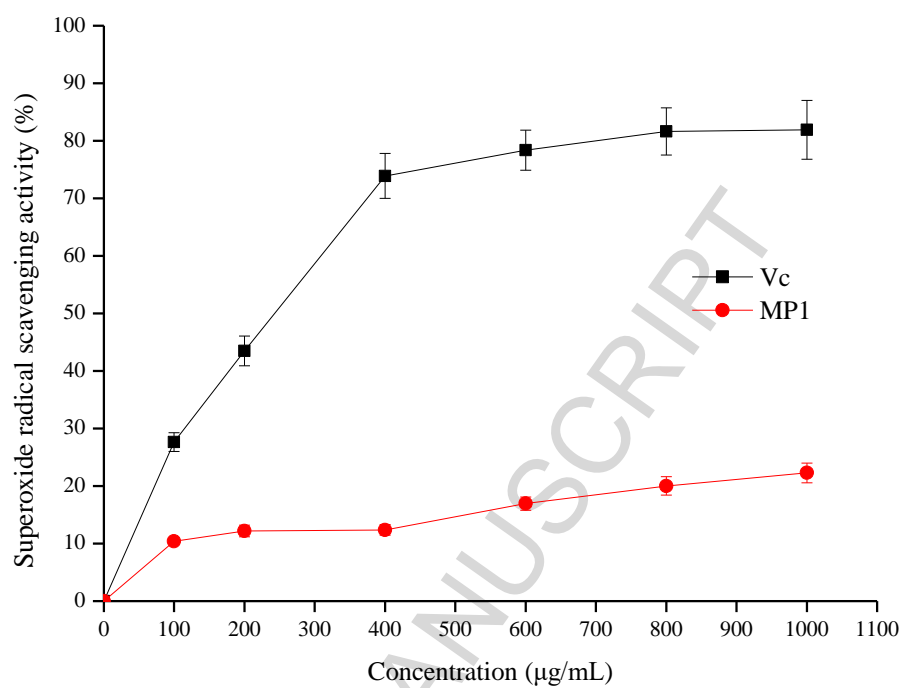
Figure 5



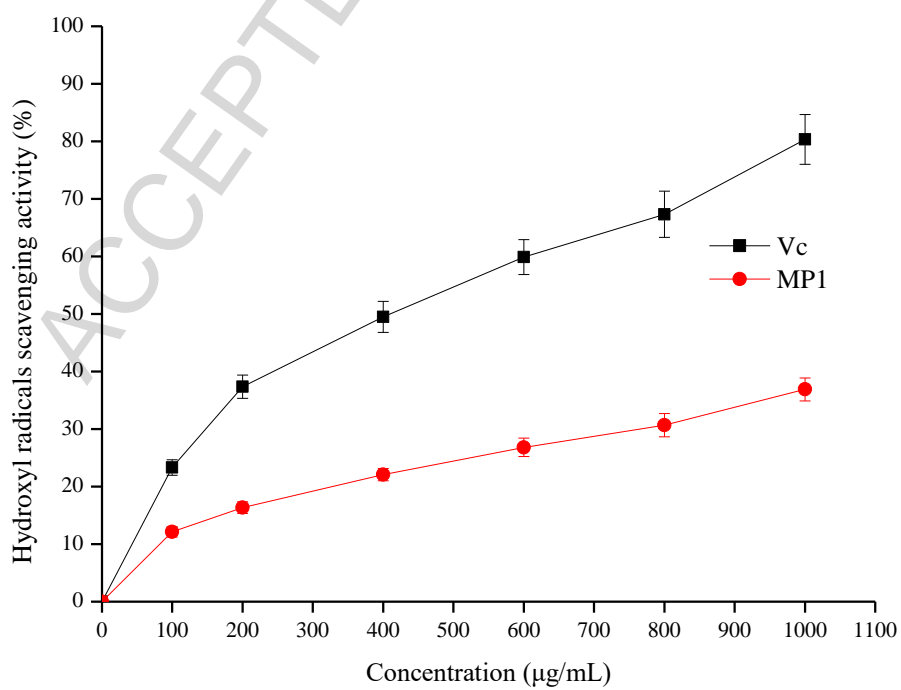
(A)



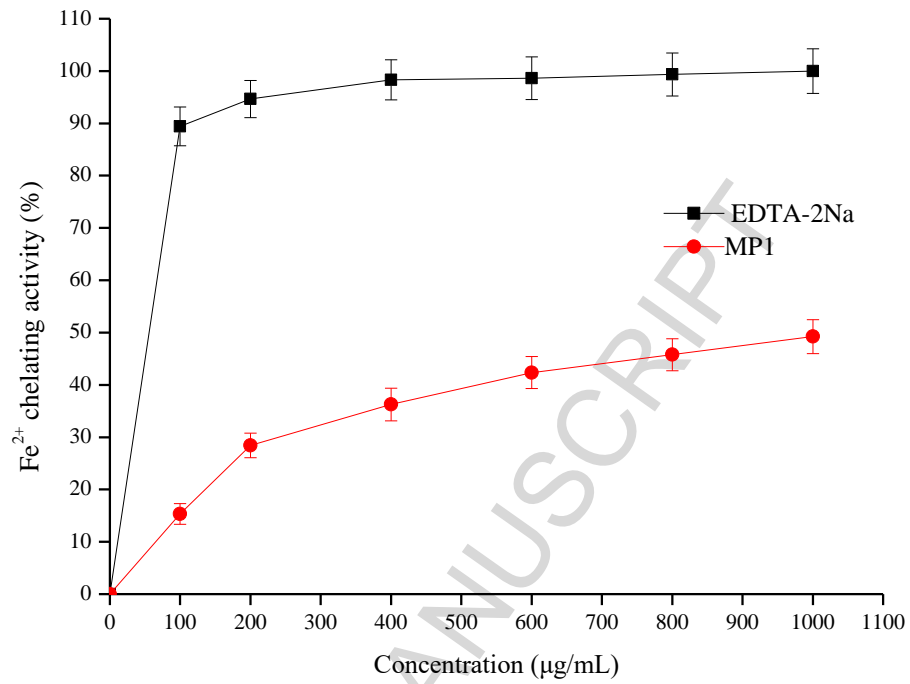
(B)



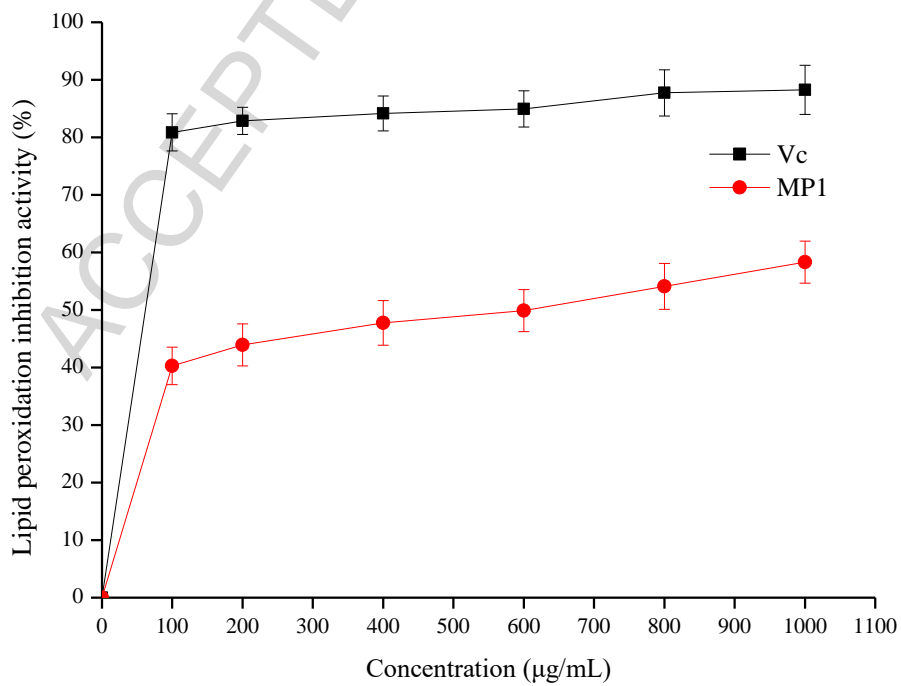
(C)



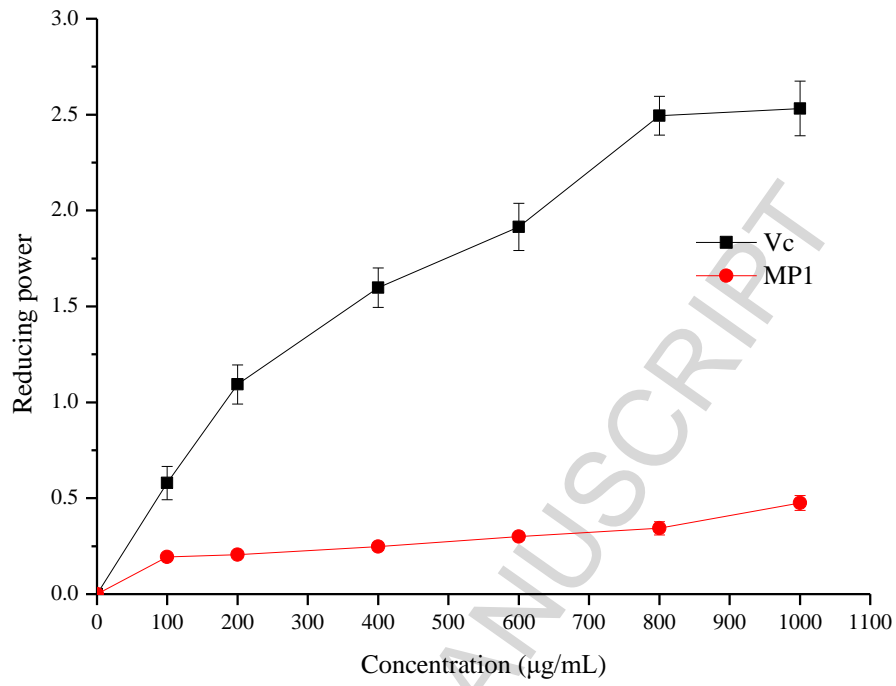
(D)



(E)

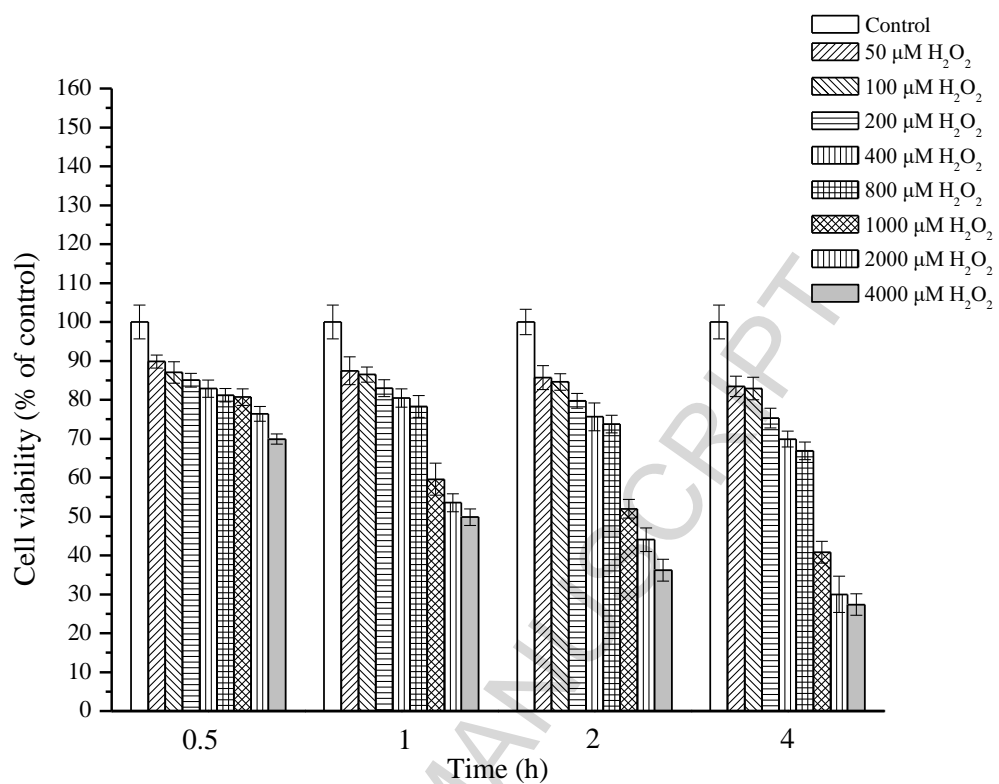


(F)

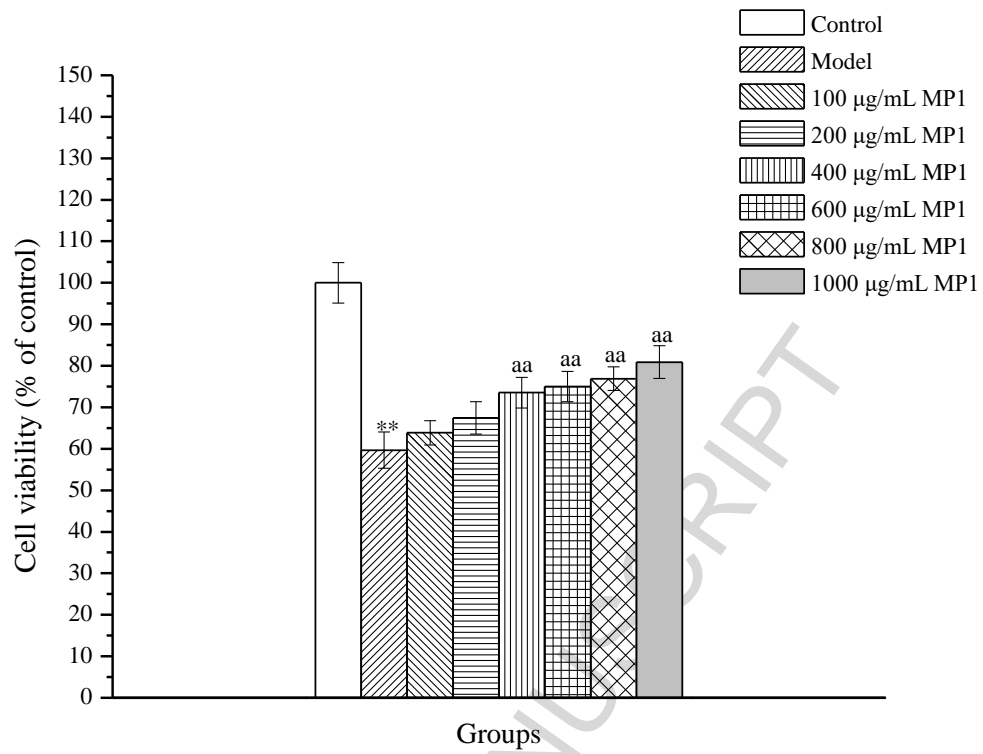


(G)

Figure 6



(A)



(B)

Figure 7

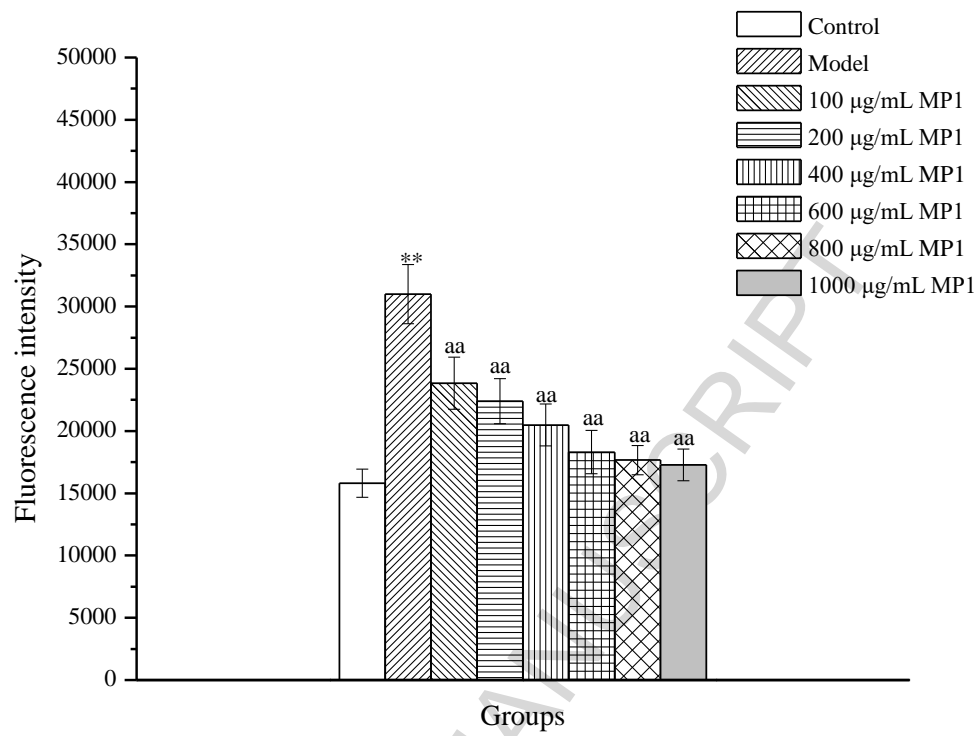
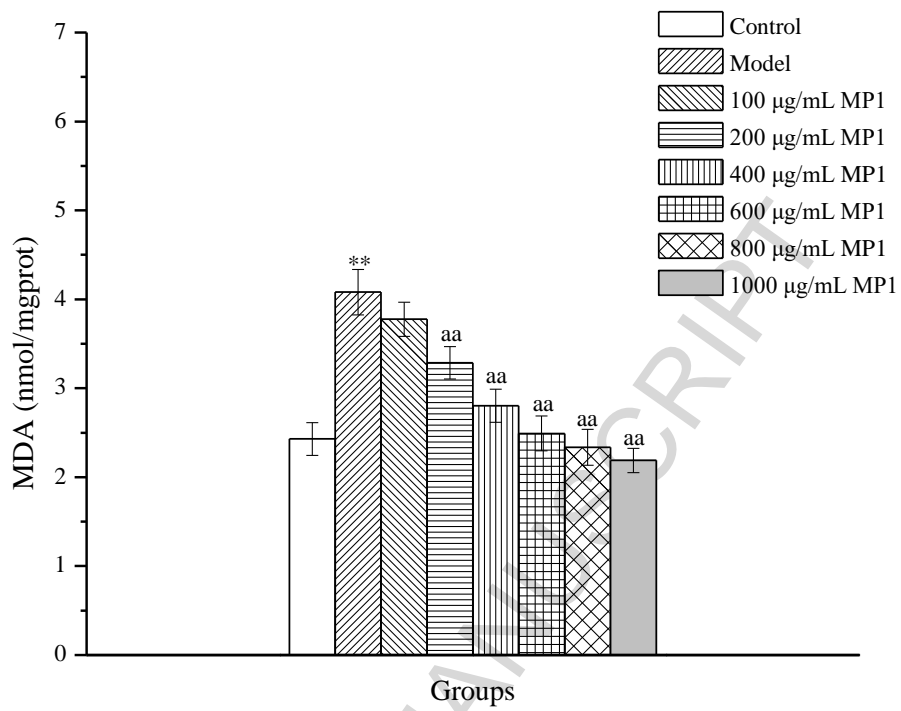
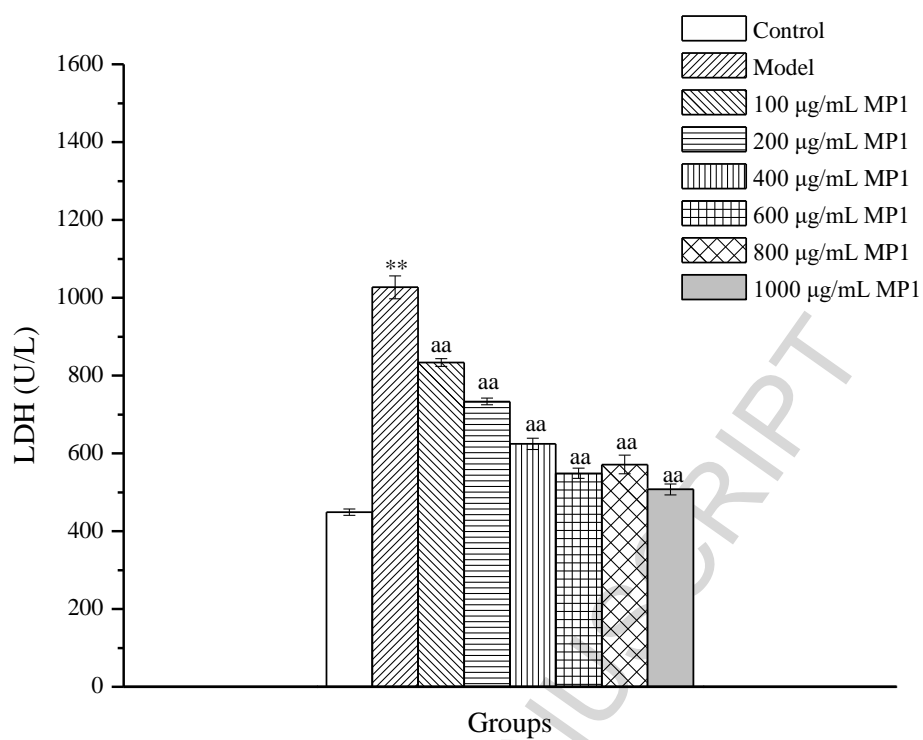


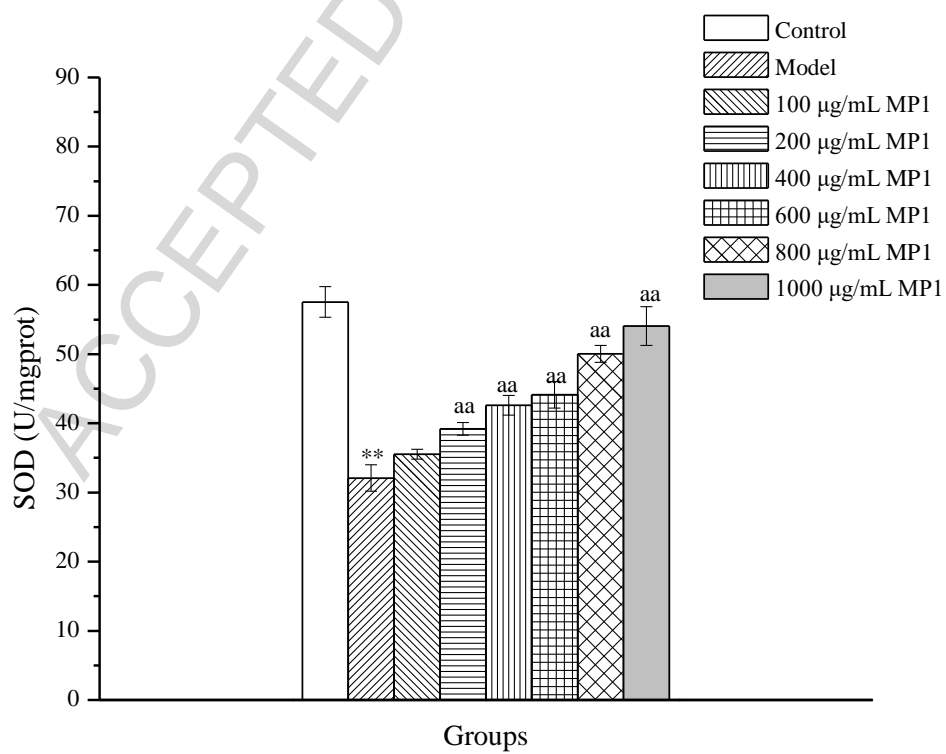
Figure 8



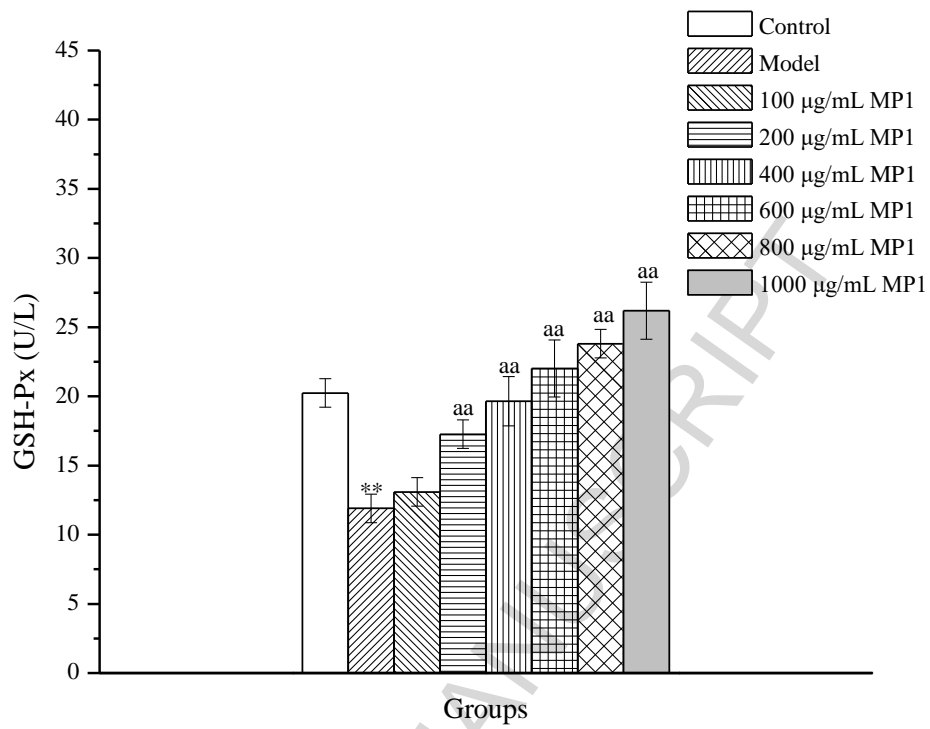
(A)



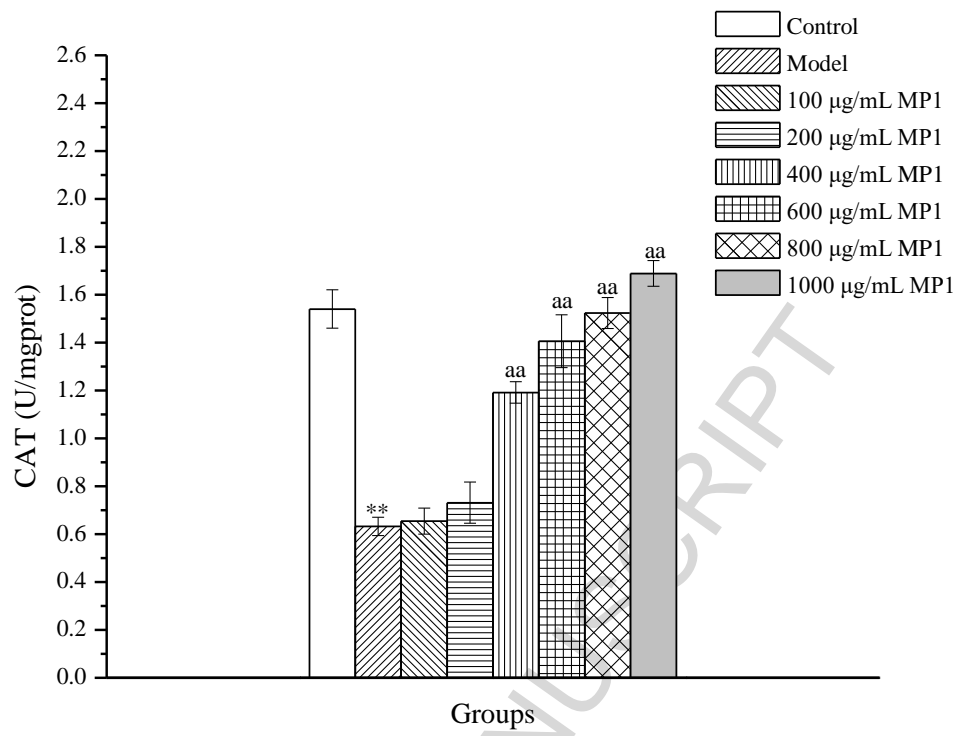
(B)



(C)



(D)



(E)

**Table 1**

Table 1 Linkage analysis of MP1

Retention time(min)	PMAA	Linkage pattern	Mass fragments (m/z)	Molar ratio
15.67	2,3,5-Me <sub>3</sub> -Ara	T-Araf	43,45,58,71,87,101,113,117,129,145,161	1.8
20.24	2,5-Me <sub>2</sub> -Ara	1,3-Araf	43,45,58,71,87,99,113,117,129,147,159,173,233	2.0
22.34	2,3-Me <sub>2</sub> -Ara	1,5-Araf	43,45,58,71,87,101,117,129,145,161,173,189	1.0
25.09	2,3,6-Me <sub>3</sub> -Gal	1,4-Galp	43,45,58,71,87,99,101,113,117,129,131,142,161,173,189,233	2.5
25.61	Ara	1,2,3,5-Araf	43,61,85,103,115,127,145,158,187,200,217,289	1.1

**Table 2**

Table 2 Chemical shift ( $\delta$ ) assignments of  $^1\text{H}$  NMR and  $^{13}\text{C}$  NMR spectra of MP1 on the basis of DQF-COSY, HSQC and HMBC.

Residues	The chemical shift of $^1\text{H}$ and $^{13}\text{C}$ (ppm)						
		1	2	3	4	5	6
(A) 1,3- $\alpha$ -Araf	H	5.33	4.39	4.05	3.93	3.80	
	C	106.01	80.96	83.61	83.47	60.52	
(B) 1,2,3,5- $\alpha$ -Araf	H	5.26	4.25	4.13	3.90	3.87	
	C	106.53	86.61	83.50	83.42	65.96	
(C) 1,5- $\alpha$ -Araf	H	5.24	4.22	4.16	4.12	3.94	
	C	106.59	80.86	76.48	83.36	65.75	
(D) T- $\alpha$ -Araf	H	5.17	4.21	4.11	4.04	3.91	
	C	107.09	81.79	76.32	83.68	60.36	
(E) 1,4- $\beta$ -Galp	H	4.72	3.77	3.81	4.14	3.78	3.92
	C	103.94	72.91	74.09	76.17	71.44	60.75

---

### Highlights

- The detailed structure of MP1 was first elucidated by GC-MS and NMR.
- The backbone was mainly consisted of arabinose and galactose residues.
- MP1 showed a moderate antioxidant activity *in vitro*.
- MP1 exhibited protective effect on the injured RAW264.7 cells induced by H<sub>2</sub>O<sub>2</sub>.
- It could be a natural antioxidant for food and pharmaceutical applications.

ACCEPTED MANUSCRIPT